american physiological society
PHYSIOLOGICAL GENOMICS

Physiol Genomics 57: 499–517, 2025.
First published June 25, 2025; doi:10.1152/physiolgenomics.00192.2024

RESEARCH ARTICLE

Embryonic hypoxia alters cardiac gene expression patterns in American alligators, Alligator mississippiensis

Turk Rhen,[1] Todd A. Castoe,[2] and Dane A. Crossley II[3]

[1]*Department of Biology, University of North Dakota, Grand Forks, North Dakota, United States;* [2]*Department of Biology, University of Texas at Arlington, Arlington, Texas, United States; and* [3]*Department of Biological Sciences, University of North Texas, Denton, Texas, United States*

Abstract

How environmental conditions during embryogenesis shape development, physiology, and phenotype is a key question for understanding the roles of plasticity and environmental factors in determining organismal traits. Answering this question is essential for revealing how early-life environmental variation drives adaptive responses and influences evolutionary processes. Here we examine how hypoxia impacts cardiac gene expression during embryonic development in the American alligator (*Alligator mississippiensis*). Eggs were incubated in normoxic (21% O_2) or hypoxic (10% O_2) conditions from 20% to 90% of embryogenesis. Embryos were sampled at 70% and 90% of development to measure gene expression, embryo mass, and organ mass. Hypoxia significantly restricted embryonic growth while enlarging hearts and brains relative to body size. Gene expression analyses show that hypoxia led to upregulation of 182 genes and downregulation of 222 genes, which were enriched in pathways related to muscle contraction, oxygen transport, protein catabolism, and metabolism. Developmental changes in 3,544 genes were associated with cell division, extracellular matrix remodeling, and structural organization. Functional and network analyses highlighted hypoxia-induced shifts in cardiomyocyte physiology, suggesting adaptations to enhance cardiac performance under low oxygen availability. Despite hypoxia-related downregulation of sarcomere and metabolic genes, hypertrophic responses were evident, consistent with previous findings of improved cardiac function in hypoxia-exposed juveniles. Collectively, our findings offer new genome-wide insights into the effects of hypoxia on the embryonic alligator heart, uncovering significant adaptive developmental plasticity. These results have broad implications for understanding how environmental factors shape cardiovascular phenotypes and drive evolutionary responses to hypoxia in reptiles.

NEW & NOTEWORTHY This study investigated the impact of hypoxia on the cardiac transcriptome in alligator embryos. Exposure to low oxygen levels induced significant changes in gene networks controlling cardiac contraction, protein catabolism, oxygen transport, pyruvate metabolism, and adrenergic signaling. Ontogenetic changes suggest slowing of cell proliferation and remodeling of the extracellular matrix in the heart as embryos approach the end of incubation. This study provides the first characterization of myocardial gene expression patterns in developing alligator hearts.

embryo; heart; hypoxia; reptile; RNA-Seq

INTRODUCTION

Environmentally induced changes in morphology, physiology, and behavior are widespread across the tree of life, enabling organisms to adapt to diverse environmental challenges (1–3). This phenotypic plasticity can be critically important for survival in fluctuating conditions (4–8). One such challenge is the availability of molecular oxygen, a key factor for most life on Earth, yet oxygen availability varies across both spatial and temporal scales (9–11). Eukaryotes have evolved a range of adaptations to sense and compensate for variation in oxygen availability, both in the external environment and within their tissues (12–14).

The respiratory and cardiovascular systems of vertebrates are prime examples of highly plastic and environmentally responsive systems that play a central role in gas exchange and delivery of oxygen to cells throughout the body (15, 16). These organ systems play a key role in homeostatic responses during periods of low oxygen availability and/or high metabolic demand for oxygen. In terrestrial vertebrates, short-term hypoxia triggers an increase in respiratory rate, heart rate, blood pressure, and cardiac output to increase oxygen delivery to cells (17, 18). These physiological parameters rapidly revert to baseline when oxygen levels return to normal. Protracted periods of hypoxia can induce acclimatization, which refers to longer-lasting changes like increased erythropoiesis, elevated

Correspondence: T. Rhen (turk.rhen@und.edu).
Submitted 17 December 2024 / Revised 3 February 2025 / Accepted 6 June 2025

hemoglobin content, and enhanced hemoglobin-O_2 affinity (19, 20). Acclimatization involves significant changes in gene expression, takes days to weeks to develop, and persists for a significant period after oxygen levels return to normal (21).

In addition to these reversible physiological effects, hypoxia can have permanent developmental effects on phenotype (12, 22–25). The developing heart of vertebrate embryos is particularly vulnerable as it is the first functional organ system during vertebrate ontogeny and must perform its transport function while continuing its organogenesis (26). Placental insufficiency in mammals restricts gas exchange, nutrient delivery, and waste removal from the fetus, which is associated with intrauterine growth restriction, low birth weight, and a higher risk of cardiovascular disease and hypertension later in life (27–29). Studies that manipulate oxygen availability alone reveal many of the effects of hypoxia on cardiovascular development are independent of other factors disrupted by placental insufficiency. Indeed, hypoxia is likely a common factor for fetal programming of cardiovascular disease in a variety of disorders that restrict placental blood flow in mammals (30).

Chronic hypoxia during embryogenesis has also been shown to influence cardiovascular development in other vertebrate groups (25). Although hypoxia causes cardiac hypertrophy in embryos of most groups and increases postnatal sympathetic tone in all groups studied so far, there are differences in its effects on other cardiovascular traits among vertebrates (25). In mammals and birds, developmental hypoxia is associated with cardiovascular dysfunction and increased susceptibility to ischemia-reperfusion injury later in life (31–33). Conversely, embryonic exposure to hypoxic conditions may preadapt some reptiles to better tolerate low oxygen levels later in life. For example, juvenile snapping turtles, *Chelydra serpentina*, exposed to hypoxia as embryos can maintain higher blood flow, stroke volume, heart rate, and cardiac power output when exposed to acute anoxia when compared with turtles that were exposed to normoxic conditions as embryos (34). Hypoxic incubation also has a lasting impact on cardiovascular phenotype in American alligators, increasing heart mass and the size of the right and left ventricular free walls and altering cardiovascular physiology in normoxic environments and in response to acute hypoxia (35–38).

In recent years, investigations of the effects of hypoxia on gene expression in developing embryonic hearts have emerged as a crucial area of research, offering insights into the adaptive physiological mechanisms used by organisms to cope with oxygen deprivation during critical stages of development (39, 40). Such functional genomic approaches have also identified hypoxia-induced changes in gene expression that program cardiovascular disease in adult mammals (41) or adaptive phenotypes in reptiles (25, 34). Here we examine the effect of developmental hypoxia on gene expression patterns in the hearts of embryonic alligators. Based on prior evidence that hypoxic incubation has significant impacts on alligator cardiovascular phenotypes (35–38), we tested the hypothesis that hypoxia induces changes in cardiac expression of genes involved in cell proliferation and apoptosis, as well as genes that play a role in cardiomyocyte function and cardiac development.

MATERIALS AND METHODS

Egg Collection and Incubation

All experiments were performed in accordance with Institutional Animal Care and Use Committee (Protocol No. 20009) at the University of North Texas. Fifteen clutches of American alligator (*Alligator mississippiensis*) eggs were collected from Rockefeller Wildlife Refuge in Grand Chenier, Louisiana, in June, 2019. Eggs were transported to the University of North Texas, weighed to the nearest milligram, and uniquely numbered. Two embryos were then dissected to determine the age of each clutch (42). Approximately equal numbers of eggs from each clutch were randomly distributed to 1-L Ziplock containers and half buried in moist vermiculite (1:1 ratio of vermiculite:water). Water content was maintained by weighing boxes three times weekly and adding water as needed. Eggs were incubated at a female-producing temperature of 30°C in a walk-in environmental chamber (Percival Scientific, Perry, IA). Alligator embryos take 72 days on average to hatch from their eggs when incubated at 30°C.

At 20% of embryogenesis (~14–15 days after oviposition), eggs were split into two treatment groups. One group was incubated in normoxic conditions (21% O_2), whereas the other group was incubated in hypoxic conditions (10% O_2) as previously described (36). In brief, egg containers were sealed inside large Ziploc bags with one hole for gas inflow and a second hole for gas outflow. Gas mixtures passed through a H_2O-bubbler to maintain high relative humidity. Normoxic gas (21% O_2; room air) or hypoxic gas (10% O_2; room air mixed with nitrogen) was pumped through bags using air pumps and rotameter flow controllers. Gas composition was monitored continuously with an oxygen analyzer (S-3AI, Applied Electrochemistry, Illinois).

Sample Collection and RNA Extraction

Embryos were sampled from each oxygen condition at 70% (~50–51 days after oviposition) and 90% (~64–65 days after oviposition) of the total incubation period. A total of 105 embryos were collected: 36 normoxic embryos at 70% of incubation, 32 hypoxic embryos at 70% of incubation, 18 normoxic embryos at 90% of incubation, and 20 hypoxic embryos at 90% of incubation. One normoxic embryo at 90% of incubation was a clear outlier for morphological measurements and was excluded from all subsequent analyses. Embryos were euthanized with an overdose of isoflurane (Isoflo; Abbott Laboratories, North Chicago, IL). Embryo mass (excluding embryonic membranes), heart mass (combined atria and ventricular mass), liver mass, lung mass, kidney mass, and brain mass were measured using an analytical balance (Mettler Toledo XS204).

All vascular elements entering and existing hearts were removed by cutting at the base of the major outflow tracts from the ventricle and the venous return to the atria. Hearts were then rinsed with heparinized saline and compressed lightly to remove excess blood and blotted dry with Kimwipes. We cannot rule out the possibility of erythrocytes in the cardiac tissue, but rinsing and blotting was done in the same way for all hearts, so we do not expect erythrocytes would contribute significantly (or differentially) to the RNA

extracted from hearts. Tissues were placed in cryotubes, flash frozen in liquid N_2, and stored at −80°C. A subset of 28 hearts from 10 clutches were shipped on dry ice to the University of North Dakota for RNA sequencing (RNA-Seq) analysis.

Frozen hearts were ground with a mortar and pestle on dry ice. Pulverized hearts were transferred to 1 mL of TRIzol reagent (Thermo Fisher Scientific) and homogenized for 30 s using a BioGen PRO200 homogenizer with a 5-mm generator probe. After homogenization, the probe was washed in fresh 100% methanol, ultrapure water, and dried with a Kimwipe to prevent cross contamination between samples. Remaining steps were carried out according to the manufacturer's RNA extraction protocol with one modification: two extra chloroform extractions were used to remove trace amounts of phenol from the aqueous phase. After RNA precipitation, RNA pellets were washed twice with 100% ethanol and resuspended in RNAse-free H_2O. The concentration of RNA was estimated with a Nanodrop spectrophotometer. Ten micrograms of RNA from each sample were treated with RNAse-free DNAse using an in-solution protocol to remove any contaminating genomic DNA (Qiagen). After DNAse treatment, RNA was repurified using the RNeasy MinElute Kit (Qiagen), and RNA concentration was measured again.

Analyses of Embryo and Organ Mass

ANOVA was used to test for oxygen and age effects on embryo mass and relative organ size (the ratio of organ to embryo mass) in all 104 embryos. RNA-Seq was used as a factor with two levels (used in RNA-Seq, $n = 28$; not used in RNA-Seq, $n = 76$) to test whether the subset of embryos in the RNA-Seq study was a representative subsample of the full set of 104 embryos. The three-way ANOVA included oxygen treatment (hypoxia vs. normoxia), embryo age (70% vs. 90% of incubation), and RNA-Seq (used vs. not used for RNA-Seq) as main effects and all interactions among these factors in a fully factorial design. Clutch was used as a blocking factor to control for potential genetic or maternal effects on embryo mass and organ size. Tukey's honestly significant difference test was used to compare relative organ sizes among four experimental groups (2 oxygen levels × 2 embryonic ages). Studentized residuals were normally distributed and homoscedastic. Thus, parametric statistics were appropriate for analyzing embryo mass and relative organ size. JMP statistical software was used to analyze morphological data.

RNA Sequencing and Analysis of Gene Expression Patterns

Total RNA was delivered to the UND Genomics Core, which assessed RNA quality using the Agilent 4200 TapeStation. RNA integrity numbers ranged from 8.8 to 9.7. The core prepared poly-A, nondirectional cDNA libraries for each of the 28 hearts. The 28 libraries were sequenced on the Nova-Seq 4000 platform to produce 22 to 30.4 million paired-end reads per sample (150 bp reads; average = 26.7 M reads/sample; 4 groups × 7 samples/group = 28 samples). FastQC (43) and MultiQC (44) were used to assess the quality of raw and trimmed reads from embryonic alligator hearts. Trimmomatic (45) was used to trim reads with the following parameters: ILLUMINACLIP:TruSeq3-PE-2.fa:2:38:10:8:TRUE HEADCROP:10 LEADING:3 TRAILING:3 SLIDINGWINDOW:4:20 MINLEN:30. After trimming, all reads (20.8 to 28.5 million paired-end reads per sample) had excellent quality control metrics.

Trimmed reads were mapped to American alligator genome assembly ASM28112v4 using HiSat2 (46). Alignment rates ranged from 94% to 95% for all samples. featureCounts was used to count the number of fragments mapped to exons (47). Genes with very low counts were prefiltered: genes had to have ≥3 counts in at least 7 samples to remain in the analysis. Principal components analysis using variance stabilized transformed (VST) counts was used to visualize relationships among experimental groups and to check for potential outliers. Differential gene expression analysis was then performed on read counts with DESeq2 (48). Oxygen treatment (normoxia vs. hypoxia), embryo age (70% vs. 90% of embryogenesis), and the oxygen treatment by age interaction were used as independent variables while using clutch identity as a blocking factor. The Wald test was used to test for oxygen treatment, embryo age, and the oxygen treatment by age interaction effects on gene expression. The Benjamini–Hochberg procedure was used to control the false discovery rate (FDR) in the transcriptome analysis. There is a tradeoff between sensitivity and specificity when selecting FDR level. We decided to prioritize sensitivity over specificity and used FDR = 0.10. However, we report adjusted P values in all our tables so readers can use more stringent FDRs if they so choose. The R packages EnhancedVolcano and Pretty Heatmaps were used for production of volcano plots and heatmaps.

Functional enrichment analyses of differentially expressed genes were carried out to gain further insights into the effects of hypoxia on heart development and physiology. Enrichment analyses were conducted using the database for annotation, visualization and integrated discovery (DAVID) (49) and the Search Tool for the Retrieval of Interacting Genes/Proteins (STRING) (50) database of protein-protein interactions with American alligator, *Alligator mississippiensis*, as the annotation reference species.

Comparative Analysis of Hypoxia-Regulated Genes

Hypoxia-regulated genes in alligator embryo hearts were compared with genes from a comprehensive meta-analysis of hypoxia-regulated genes in human and mouse (51). Lists of genes were downloaded for human (https://doi.org/10.6084/m9.figshare.5812710.v3) and for mouse (https://doi.org/10.6084/m9.figshare.9948233.v2). Lists were filtered to identify the top 2.5% of genes in each tail of the hypoxia and normoxia scores (HN scores). The authors define the HN score for a gene as the count of RNA-Seq studies in which the gene was significantly upregulated by hypoxia minus the count of RNA-Seq studies in which the gene was significantly downregulated by hypoxia (51). Thus, genes with positive HN scores were upregulated in more studies than they were downregulated, whereas negative HN scores indicate the opposite (see Ref. 51 for further details). Venny 2.1 (52) was used to compare hypoxia-regulated genes in alligators with hypoxia-regulated genes in human and mouse.

RESULTS

Embryo Mass and Relative Organ Size

Incubation of eggs in hypoxic conditions inhibited growth of alligator embryos and this effect became more pronounced

with age, as indicated by a significant oxygen treatment by age interaction (Table 1; Fig. 1*A*). Although the absolute mass of hearts was smaller in hypoxic embryos compared with normoxic embryos, hearts from hypoxic embryos were significantly enlarged relative to their body size (Table 1; Fig. 1*B*). The effect of hypoxia on relative heart size was similar at both ages; i.e., there was no detectable oxygen treatment by age interaction (Table 1; Fig. 1*B*). Overall, there was negative allometry between heart and body size; i.e., relative heart size decreased from 70% to 90% of embryogenesis in both normoxic and hypoxic conditions (Table 1; Fig. 1*B*). There was no difference in total embryo mass or relative heart size between embryos used for RNA-Seq and embryos that were not used for RNA-Seq (Table 1). Likewise, interactions among RNA-Seq, oxygen treatment, and embryo age were not significant (Table 1). These results indicate that the 28 embryos used for RNA-Seq were a representative subsample of the entire set of 104 embryos.

Although hypoxia caused cardiac enlargement (i.e., hypoxic hearts were enlarged relative to body size), the impact of hypoxia on other organs varied. Brains of hypoxic embryos were enlarged relative to body size much like heart size (Table 1; Fig. 1*C*). Negative allometry was also observed for brain size; i.e., relative brain size decreased from 70% to 90% of incubation in both normoxic and hypoxic conditions (Table 1; Fig. 1*C*). In contrast, hypoxia had no impact on the relative size of kidneys or livers, which both scaled isometrically with body size (Table 1; Fig. 1, *D* and *E*). Finally, relative lung size was smaller in hypoxic embryos compared with normoxic embryos at 70% of embryogenesis, but there was no difference at 90% of embryogenesis (Table 1; Fig. 1*F*). Lung size displayed negative allometry like brain and heart size; i.e., relative lung size decreased from 70% to 90% of embryogenesis in both oxygen conditions (Table 1; Fig. 1*F*). There were no differences in relative organ sizes between embryos used for RNA-Seq and embryos that were not used for RNA-Seq (Table 1). Interactions among RNA-Seq, oxygen treatment, and embryo age were not significant for any organ (Table 1). These results again indicate the 28 embryos used for RNA-Seq were a representative subsample from the full set of embryos.

Identification of Differentially Expressed Genes

The dispersion plot for normalized read counts of all genes was examined both before and after shrinkage with the DESeq2 algorithm. Dispersion decreased as gene expression levels increased, with the fitted dispersion showing a smooth monotonic function typical of high-quality data (Fig. 2*A*). In addition, there was relatively little shrinkage of dispersion values because sample sizes were moderate ($n = 7$ samples/group). Expression of all genes was also visualized with a PCA plot. The first principal component captured 26% of the variance in gene expression, and samples were primarily clustered by embryo age (Fig. 2*B*). The second principal component captured 17% of the variance with slight separation of normoxic and hypoxic groups at 90% of embryogenesis (Fig. 2*B*). Other components did not distinguish treatment groups.

DESeq2 was then used to test for differences in gene expression between oxygen treatments (normoxia vs. hypoxia), between ages (70% vs. 90% of embryogenesis), and for an oxygen treatment by age interaction. At a Benjamini–Hochberg-adjusted FDR of 0.1, hypoxia treatment upregulated 182 genes and downregulated 222 genes (Fig. 3*A*; Supplemental Table S1). The 20 genes most highly upregulated and downregulated (in magnitude) by hypoxia are shown in Table 2. Age had a much larger effect on the transcriptome with 1,960 genes upregulated and 1,584 genes downregulated in embryos at 90% of embryogenesis compared with embryos at 70% of embryogenesis (Fig. 3*B*; Supplemental Table S2). The 20 genes that changed the most developmentally are shown in Table 3. A total of 65 genes displayed a significant interaction between oxygen treatment and age (Fig. 3*C*; Supplemental Table S3). The 20 genes that display the strongest oxygen treatment by age interaction are shown in Table 4.

Several positive control genes known to be regulated by hypoxia in humans and mice were also hypoxia-regulated in alligator heart (Fig. 4). See *Comparative Analysis of Hypoxia-Regulated Genes* below for more genes that are shared among these species. Several positive control genes known to play important roles in heart development late in embryogenesis in other species were also developmentally regulated in alligator (Fig. 5).

A heatmap of differentially expressed genes is shown in Fig. 6, which includes genes affected by oxygen treatment, age, or the oxygen treatment by age interaction. Hierarchical clustering showed the greatest difference in gene expression patterns between hearts at 70% and 90% of embryogenesis (i.e., the deepest branch in the dendrogram in Fig. 6). In

Table 1. *ANOVA results for the effects of oxygen condition, age, and the oxygen condition by age interaction on embryo mass and relative organ sizes (i.e., organ mass/embryo mass)*

		Embryo Mass		Heart Mass / Embryo Mass		Brain Mass / Embryo Mass		Kidney Mass / Embryo Mass		Liver Mass / Embryo Mass		Lung Mass / Embryo Mass	
Factors	df	*F*	*P*	*F*	*P*	*F*	*P*	*F*	*P*	*F*	*P*	*F*	*P*
Oxygen condition	1	137.8	<0.0001	33.6	<0.0001	34.5	<0.0001	0.01	0.92	2.48	0.12	21.4	<0.0001
Age	1	262.8	<0.0001	44.4	<0.0001	55.2	<0.0001	1.21	0.27	0.24	0.62	129.3	<0.0001
Oxygen condition × age interaction	1	36.2	<0.0001	0.97	0.33	0.22	0.64	0.18	0.67	0.01	0.91	5.1	0.026
RNA-Seq	1	2.5	0.12	0.97	0.33	0.01	0.91	0.48	0.49	3.47	0.07	1.22	0.27
Oxygen condition × RNA-Seq	1	0.2	0.70	2.8	0.10	0.58	0.45	0.00	0.96	0.38	54	0.51	0.48
Age × RNA-Seq	1	0.6	0.44	0.04	0.85	1.6	0.21	0.26	0.61	0.11	0.74	1.38	0.24
Oxygen condition × Age × RNA-Seq	1	2.9	0.09	3.5	0.06	0.33	0.57	0.11	0.74	0.8	0.37	1.39	0.24
Clutch ID	14	2.70	0.0026	1.88	0.04	1.92	0.04	2.22	0.01	1.88	0.04	3.05	0.0008

We also tested for differences between the subset of samples used for RNA-Seq and samples that were not, as well as the interaction with oxygen condition and age in a fully factorial model. Clutch identity was used as a blocking factor to control for potential genetic and/or maternal effects on offspring and organ size. df, degrees of freedom; *F*, *f*-statistic; *P*, probability; RNA-Seq, RNA sequencing.

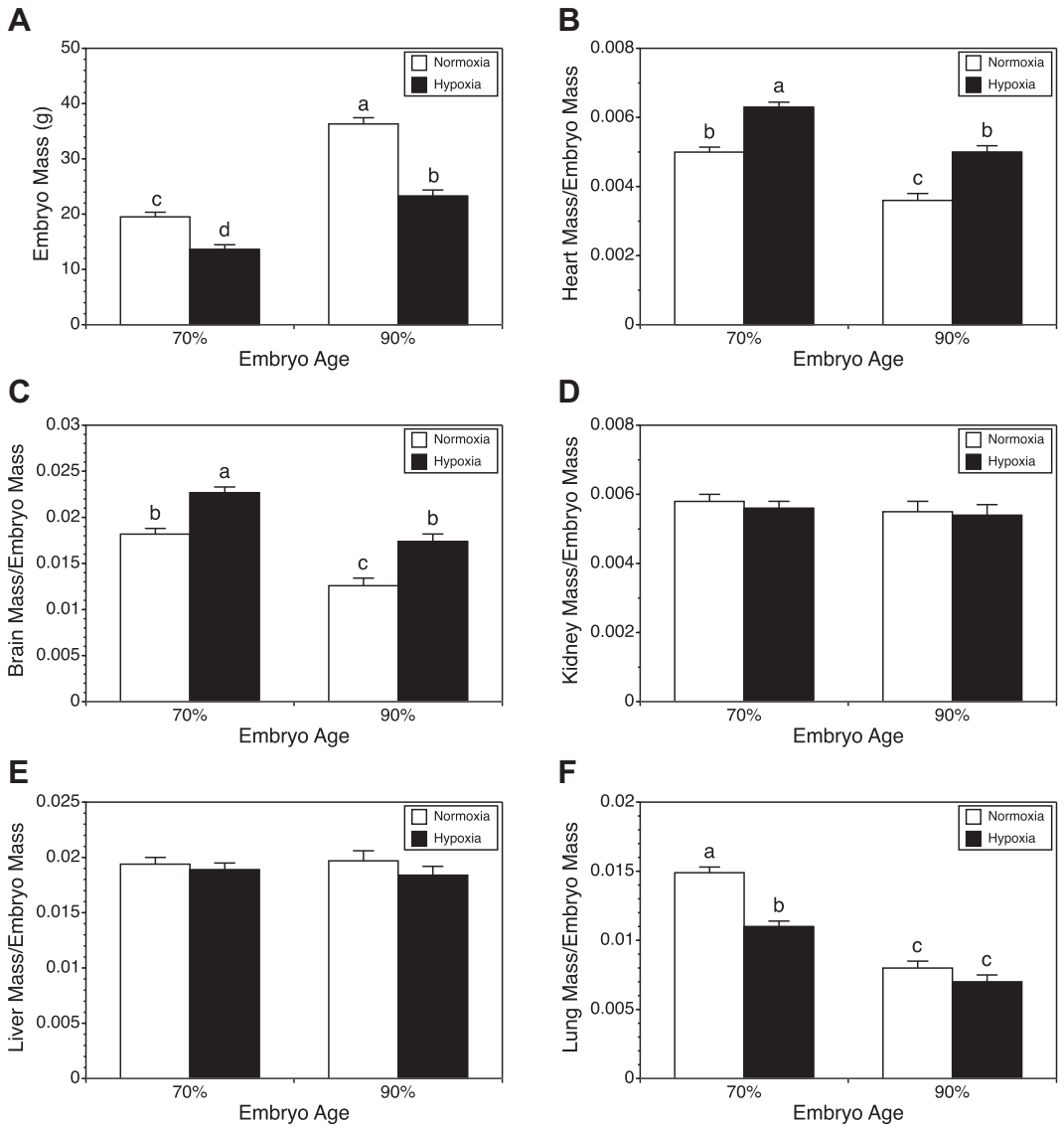

Figure 1. Oxygen availability influences growth of alligator embryos and has organ-specific effects. *A*: total mass of alligator embryos incubated in normoxic (21% O_2) or hypoxic (10% O_2) conditions from 20% of embryogenesis to 70% or 90% of embryogenesis. Other panels show the mass of various organs relative to embryo mass: relative heart mass (*B*), relative brain mass (*C*), relative kidney mass (*D*), relative liver mass (*E*), and relative lung mass (*F*) of these embryos. Embryo mass and relative mass of organs are means ± SE. Samples sizes for 70% Normoxia ($n = 36$), 70% Hypoxia ($n = 32$), 90% Normoxia ($n = 19$), 90% Hypoxia ($n = 20$). Tukey's Honestly Significant Difference Test was carried out after ANOVA indicated significant main effects of oxygen treatment or age. Different letters indicate groups that significantly differ from each other for a given trait (groups with the same letter do not differ).

contrast, there was not clear clustering by oxygen treatment (i.e., hypoxic and normoxic groups were not completely separated within each age category).

Functional Enrichment of Differentially Expressed Genes

DAVID was used to test for functional enrichment among genes affected by oxygen treatment or the oxygen treatment by age interaction. Of 454 genes in this list, 391 genes were in the DAVID database for American alligator. There was enrichment among these genes at an unadjusted P value $<$ 0.05 (Fig. 7), but not with a more stringent FDR threshold. Differentially expressed genes related to muscle fiber structure and contraction were enriched in four out of five databases (Fig. 7, *A*, *B*, *D*, and *E*). Genes related to the proteasome and apoptosis were enriched in three out of five databases (Fig. 7, *A*, *B*, and *D*). Genes related to oxygen transport and oxygen binding were enriched in three out of five databases (Fig. 7, *A*, *C*, and *E*). Genes involved in synaptic transmission/adrenergic signaling were enriched in two databases (Fig. 7, *A* and *D*). Other functional categories of genes were only enriched in single databases.

Out of 3,544 genes differentially expressed between hearts at 70% and 90% of embryogenesis, 3,087 genes were in the DAVID database for American alligator. There was functional enrichment among these genes at a stringent FDR threshold $<$ 0.05 (Fig. 8). Differentially expressed genes were more likely to be involved in cell division, mitosis, and associated with the centromere than expected by chance in four of five databases (Fig. 8, *A*, *B*, *D*, and *E*). Genes associated with microtubules and

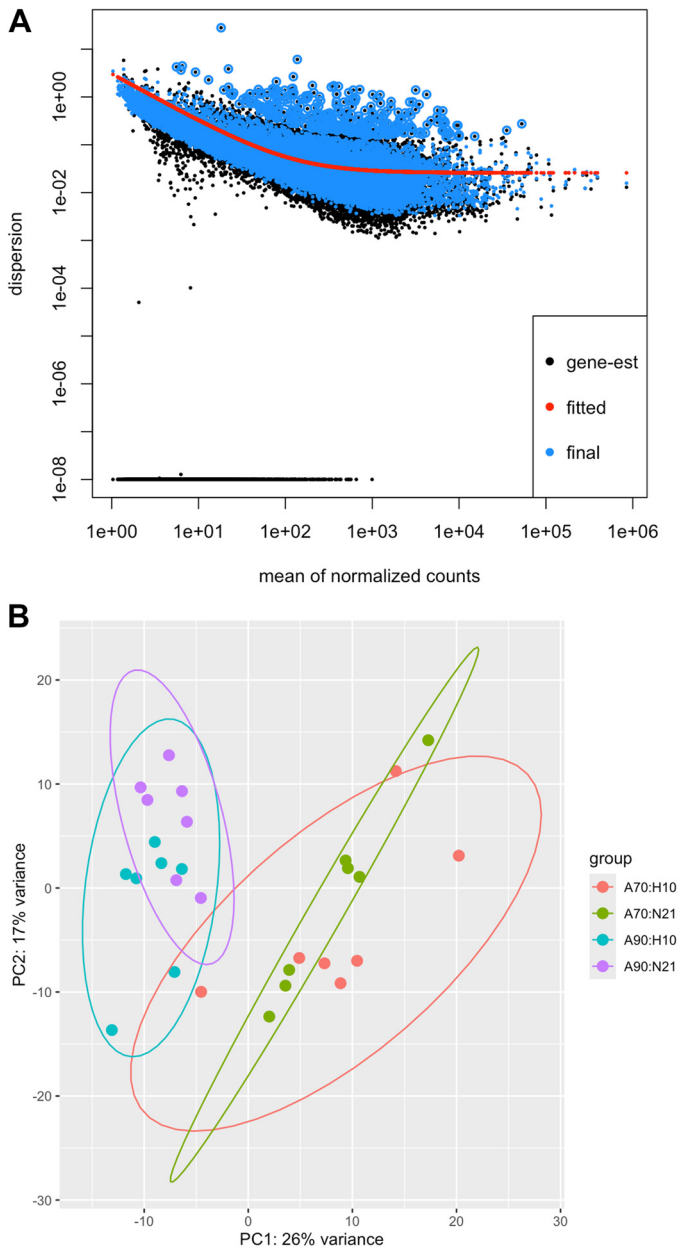

Figure 2. Quality control assessment of RNA sequencing (RNA-Seq) data. *A*: plot of gene-wise dispersion estimates vs. average expression level before (black dots) and after (blue dots) shrinkage of gene-wise dispersion estimates toward the fitted curve (red dots) for the entire transcriptome. *B*: principal component analysis plot showing the first two principal components (PC1 and PC2) and 95% confidence ellipses for variance-stabilized gene expression values. The key next to the plot shows the 4 treatment groups: A70-H10 = 70% of embryogenesis and hypoxia, A70-N21 = 70% of embryogenesis and normoxia, A90-H10 = 90% of embryogenesis and hypoxia, and A90-N21 = 90% of embryogenesis and normoxia. Samples sizes for 70% Normoxia ($n = 7$), 70% Hypoxia ($n = 7$), 90% Normoxia ($n = 7$), 90% Hypoxia ($n = 7$).

microtubule-based movement were enriched in four out of five databases (Fig. 8, *A–C,* and *E*). Finally, genes associated with the extracellular matrix, extracellular matrix receptors, and basement membrane were enriched in four out of five databases (Fig. 8, *A, B, D,* and *E*). Other functional categories of genes were only enriched in one or two databases.

Network Analysis of Hypoxia Regulated Genes

The STRING database was used for network analysis of genes affected by oxygen treatment or the oxygen treatment by age interaction. Of 454 genes in this list, 296 were in the String database for American alligator. We used the Markov Cluster Algorithm (MCL) with an inflation parameter of 3 to identify clusters of genes enriched for protein-protein interactions in the network graph ($P < 1.0e-16$ for PPIs in clusters 1–4 and $P < 1.8e-07$ for cluster 5; Fig. 9).

The largest cluster of 17 genes was enriched for genes that function in "proteolysis involved in protein catabolic process" ($P < 5.97e-11$; Fig. 9). More of these genes were downregulated by hypoxia than expected if there were an equal chance of being upregulated or downregulated (15 genes downregulated and 2 genes upregulated; $P = 0.002$).

The next largest cluster of 15 genes was enriched for genes that contain "tetratricopeptide repeats" ($P = 0.004$; Fig. 9). This cluster was not enriched for any biological process. There were similar numbers of upregulated and downregulated genes in this cluster with no bias in expression pattern (8 genes downregulated and 7 genes upregulated; $P = 1.0$).

The third largest cluster of 11 genes was enriched for genes that are part of the "myosin II complex and troponin complex" ($P < 4.1e-14$; Fig. 9). More of these genes were downregulated by hypoxia than expected by chance (10 genes downregulated and 1 gene upregulated; $P = 0.01$).

The fourth largest cluster of 8 genes was enriched for genes involved in "pyruvate metabolism and citric acid cycle" ($P < 5.1e-09$; Fig. 9). Exposure to hypoxia tended to downregulate expression of these genes (7 genes downregulated and 1 gene upregulated; $P = 0.07$).

The last cluster of 5 genes was enriched for genes with "translation initiation factor activity" ($P < 1.2e-07$; Fig. 9). Four of these genes were upregulated by hypoxia, whereas one gene was downregulated, which is not different from an even ratio ($P = 0.375$). Clusters with less than 5 genes were not considered large enough for functional enrichment analysis.

Network Analysis of Developmentally Regulated Genes

Given the extremely large number developmentally regulated genes, a more stringent threshold (FDR < 0.05 and > 1.5-fold change) was used to produce a shorter list of genes for network analysis. Of 1,608 genes in this list, 1,020 were in the String database for American alligator. We used the Markov cluster algorithm (MCL) with an inflation parameter of 3 to identify clusters of genes enriched for protein-protein interactions: only genes in the top five clusters are shown for clarity ($P < 1.0e-16$ for PPIs in clusters 1–5; Fig. 10).

The largest cluster of 99 genes was enriched for genes that function in "cell division" ($P < 1.71e-59$; Fig. 10). More of these genes were downregulated at 90% compared with 70% of embryogenesis than expected if there were an equal chance of being upregulated or downregulated (97 genes downregulated and 2 genes upregulated; $P < 1e-12$).

The second largest cluster of 21 genes was enriched for genes that function in the "RHOA GTPase cycle" ($P < 1.58e-10$; Fig. 10). More of these genes were upregulated at 90% compared with 70% of embryogenesis than expected if there were an equal chance of being upregulated or

Figure 3. Volcano plots for cardiac gene expression in alligator embryos. The *x*-axis represents the log2 fold change in expression, whereas the *y*-axis displays the negative log10 of the *P* value for comparisons between oxygen treatment groups (*A*), embryos at different ages (*B*), and the interaction between oxygen treatment and age (*C*). Points shown in red are differentially expressed using the thresholds described in RESULTS.

downregulated (5 genes downregulated and 16 genes upregulated; $P = 0.027$).

The third largest cluster of 19 genes was enriched for genes that function in "DNA replication" ($P < 5.72\text{e-}16$; Fig. 10). More of these genes were downregulated at 90% compared with 70% of embryogenesis than expected if there were an equal chance of being upregulated or downregulated (18 genes downregulated and 1 gene upregulated; $P = 0.00008$).

Table 2. *The top 20 genes that are differentially expressed between oxygen treatments*

Gene Symbol	Base Mean	log2FC	lfcSE	Stat	*P* Value	*P* adj	
LOC109286192	81.47	1.62	0.36	4.52	6.16e-06	0.006117052	Higher in hypoxia
FAM19A1	18.32	1.58	0.40	3.97	7.33e-05	0.018192513	
LOC109280256	25.08	1.46	0.43	3.39	0.000690151	0.055307018	
nbis-pseudo87	29.36	1.44	0.35	4.11	3.93e-05	0.015804063	
LOC109284543	14.90	1.41	0.41	3.44	0.000583247	0.050096149	
LOC106737547	17.56	1.37	0.42	3.27	0.001076809	0.064812495	
LOC106739775	31.07	1.31	0.35	3.79	0.000152875	0.028918888	
LOC102557688	380.34	1.21	0.37	3.30	0.000980535	0.062322795	
LOC109281159	40.28	1.21	0.33	3.61	0.000300592	0.03760039	
LOC106739233	43.07	1.18	0.27	4.40	1.07e-05	0.00809276	
CHRM3	20.35	1.15	0.38	3.03	0.002440241	0.098933282	
LOC102565680	40.14	1.12	0.34	3.30	0.00097029	0.06216897	
CFAP69	17.30	1.11	0.31	3.64	0.000267553	0.035997116	
CCDC102B	16.88	1.11	0.31	3.56	0.000369699	0.04079531	
LOC102573476	85.40	1.11	0.34	3.30	0.000977839	0.062322795	
LOC109283964	14.01	1.10	0.33	3.34	0.000848387	0.059914984	
GLDC	115.57	1.09	0.31	3.53	0.000419667	0.043871732	
LOC106737515	102.98	1.08	0.25	4.24	2.19e-05	0.012687796	
LOC109280291	24.30	1.08	0.33	3.24	0.00175624	0.069703976	
MEIKIN	18.82	1.04	0.33	3.18	0.001485591	0.079039908	
LOC109286105	35.89	−0.97	0.24	−3.98	7.00e-05	0.017929668	
LOC102565495	427.09	−0.97	0.28	−3.50	0.000459614	0.045556691	
RHOH	30.33	−0.98	0.31	−3.20	0.001388633	0.077151661	
ACTG2	1,745.47	−1.04	0.18	−5.77	7.74e-09	0.000122913	
LOC106738987	44.56	−1.04	0.34	−3.08	0.002080958	0.092107037	
LOC102566837	36.13	−1.07	0.33	−3.22	0.001294398	0.073720396	
nbisL1-trna-22	339.69	−1.09	0.29	−3.74	0.000187035	0.032304159	
SLC39A8	83.82	−1.14	0.27	−4.27	1.94e-05	0.012348006	
LOC102557980	115.08	−1.14	0.34	−3.36	0.000770267	0.05762848	
LOC102575298	13.95	−1.14	0.34	−3.37	0.000760329	0.0572858	
AMH	79.91	−1.15	0.22	−5.16	2.45e-07	0.001299236	
LOC102576972	9,465.06	−1.31	0.39	−3.36	0.000785521	0.057786692	
LOC109284673	44.13	−1.31	0.38	−3.48	0.000505943	0.046470736	
LOC102560255	457.76	−1.41	0.39	−3.61	0.000307618	0.03760039	
TAGAP	31.03	−1.44	0.46	−3.12	0.001801014	0.086192415	
TMEM252	405.43	−1.48	0.36	−4.09	4.29e-05	0.016091919	
GREM2	18.73	−1.66	0.38	−4.37	1.24e-05	0.00884032	
LOC102566807	35.45	−1.75	0.39	−4.44	9.00e-06	0.007526913	
LOC109283326	21.97	−1.94	0.52	−3.70	0.000214867	0.03390983	
SLN	13.85	−2.02	0.55	−3.64	0.000271847	0.035997116	Higher in normoxia

See Supplemental Table S1 for gene IDs and products of LOC-coded genes. lfcSE, log2FC standard error.

Table 3. *The top 20 genes that are differentially expressed between developmental stages*

Gene Symbol	Base Mean	log2FC	lfcSE	Stat	*P* Value	*P* adj	
ALB	137.27	8.70	2.33	3.74	0.00018679	0.003664888	Higher 90%
LOC109281535	5.38	5.13	1.01	5.08	3.87e-07	2.74e-05	
LOC102576694	16.25	5.12	0.87	5.88	4.00e-09	6.12e-07	
ATP13A4	64.93	4.60	0.80	5.77	7.84e-09	1.04e-06	
LOC106738064	6.56	4.51	0.96	4.68	2.85e-06	0.000144066	
LOC109283555	19.85	4.09	0.50	8.16	3.48e-16	3.58e-13	
LOC102569228	10.57	3.99	0.67	5.96	2.49e-09	3.91e-07	
LOC106738279	7.39	3.98	1.00	3.97	7.12e-05	0.001807134	
ATP13A5	3.85	3.97	1.13	3.51	0.000446887	0.007030871	
LOC109284527	74.65	3.89	0.73	5.31	1.10e-07	9.19e-06	
LOC106738201	37.35	3.65	0.51	7.23	4.91e-13	2.02e-10	
LOC102560408	63.10	3.63	0.51	7.08	1.42e-12	5.24e-10	
LOC106738408	10.89	3.63	0.68	5.35	9.01e-08	7.86e-06	
LOC102562759	6.98	3.60	0.95	3.80	0.000143405	0.003015097	
LOC102561117	32.54	3.59	0.66	5.41	6.34e-08	5.92e-06	
TMEM213	4.29	3.56	1.02	3.50	0.000460609	0.007185327	
LOC102576790	2.75	3.56	1.22	2.92	0.00351341	0.030418866	
MARVELD3	5.04	3.55	0.83	4.27	1.92e-05	0.000645534	
LOC106737518	505.10	3.52	0.64	5.50	3.85e-08	3.90e-06	
LOC102562523	104.48	3.44	0.87	3.96	7.64e-05	0.001891626	
S100Z	4.98	−2.12	0.70	−3.01	0.002575646	0.024438255	
CCNA1	6.00	−2.14	0.65	−3.31	0.000939007	0.012098545	
GABRG1	419.85	−2.19	0.30	−7.23	4.91e-13	2.02e-10	
SYPL1	4.71	−2.21	0.74	−2.98	0.002861577	0.02642424	
LOC109284494	3.12	−2.23	0.89	−2.51	0.012005712	0.072245347	
LOC109285763	2.75	−2.24	0.87	−2.57	0.010129546	0.064581963	
CCDC190	6.82	−2.25	0.64	−3.50	0.000462016	0.007195471	
LOC109280291	24.30	−2.27	0.43	−5.33	9.97e-08	8.46e-06	
SCN4A	8.35	−2.30	0.57	−4.03	5.56e-05	0.001481178	
RHOV	22.53	−2.32	0.59	−3.92	8.95e-05	0.002107114	
LOC102570601	3.84	−2.34	0.98	−2.39	0.016752646	0.090524958	
LOC102565396	3.04	−2.53	1.04	−2.43	0.015079305	0.08426376	
CA6	4.01	−2.57	1.03	−2.50	0.012446515	0.07404747	
SELE	600.74	−2.57	0.87	−2.94	0.003250763	0.028791583	
DRD1	27.60	−2.73	0.56	−4.91	9.00e-07	5.55e-05	
VCAM1	959.03	−2.75	0.50	−5.46	4.65e-08	4.57e-06	
LOC109283403	3.42	−2.95	0.99	−2.97	0.002937394	0.026910026	
LOC102569407	718.66	−3.37	1.08	−3.11	0.00188271	0.019713585	
LOC102558077	5.99	−3.49	1.26	−2.78	0.005458903	0.041943781	
LOC109281253	2.76	−3.85	1.16	−3.31	0.000932242	0.012036526	Lower 90%

See Supplemental Table S2 for gene IDs and products of LOC-coded genes. lfcSE, log2FC standard error.

The fourth largest cluster of 15 genes was enriched for genes that function in the "extracellular matrix" ($P < 8.1e-10$; Fig. 10). The genes in this cluster did not show a significantly biased expression pattern, though there was a tendency toward upregulation (4 genes downregulated and 11 gene upregulated; $P = 0.12$).

The last cluster of 12 genes was enriched for genes that play a role in "blood vessel morphogenesis" ($P < 1.2e-8$; Fig. 10). However, there was no detectable bias in the pattern of expression of these genes (4 genes downregulated and 8 gene upregulated; $P = 0.38$).

Comparative Analysis of Hypoxia-Regulated Genes

There were 2,035 genes in the two tails (top 2.5% in each tail) of the HN scores for RNA-Seq studies in humans and 1,353 genes in mice. A total of 451 alligator genes were affected by oxygen treatment or the oxygen treatment by age interaction. There were 273 genes affected by hypoxia in two or more of these species (Supplemental Table S4). Only 11% (224/2,035) of the human genes were also among the top hypoxia-regulated genes in mice. Conversely, 16.5% (224/1,353) of the hypoxia-regulated genes in mice were also hypoxia-regulated in humans. Of the alligator genes, 6.9% (31/451) were hypoxia-regulated in humans. A similar percentage of alligator genes (6.3%, 28/451) were hypoxia-regulated in mice. *AIMP2*, *BAG2*, *SEC61G*, *SIAH2*, and *TPI1* were universally influenced by hypoxia in all three species and *EDN2* in alligators and humans (Fig. 4).

DISCUSSION

This study demonstrates that hypoxia significantly alters cardiac gene expression and growth in American alligator embryos (*Alligator mississippiensis*). These findings align with a growing body of evidence that developmental hypoxia induces both immediate and long-term cardiovascular changes in vertebrates (25, 53). There were also extensive developmental changes in gene expression patterns in hearts between 70% and 90% of embryogenesis. These results build on previous work show that hypoxia induces changes in cardiovascular development and physiology in alligators (35–38, 54). Our findings provide insights into how chronic oxygen deprivation shapes cardiovascular phenotypes at the level of gene expression, particularly in species that experience hypoxic conditions during critical periods of development.

Table 4. *The top 20 genes that display a significant oxygen treatment by age interaction*

Gene Symbol	Base Mean	log2FC	lfcSE	Stat	*P* Value	*P* adj
LOC106737891	10.16	4.19	1.02	4.11	3.88e-05	0.044827627
LOC109282749	37.72	1.79	0.47	3.82	0.000133717	0.070686605
IBSP	26.90	1.49	0.41	3.59	0.000326974	0.096026563
TNFSF11	19.44	1.43	0.40	3.59	0.000334274	0.096636443
LOC106738458	27.35	1.28	0.34	3.71	0.00020677	0.086554107
P2RX5	820.30	1.00	0.25	3.97	7.17e-05	0.052927668
WNK4	1,266.83	0.89	0.18	4.98	6.23e-07	0.005763737
nbisL1-trna-20	5,074.47	0.88	0.21	4.14	3.55e-05	0.044827627
PTGIS	7,437.71	0.86	0.23	3.80	0.000143689	0.071673525
CDK10	161.90	0.83	0.21	3.94	8.02e-05	0.05467074
DNAAF5	285.10	0.79	0.20	3.94	8.27e-05	0.05467074
GPAT4	3,679.02	0.77	0.21	3.62	0.000299831	0.094923511
LOC102572264	2881.87	0.77	0.17	4.40	1.07e-05	0.025834059
LOC109281412	105.04	0.76	0.18	4.10	4.12e-05	0.044854956
nbis-6	369,713.14	0.73	0.17	4.27	1.93e-05	0.034228732
nbis-11	41,339.70	0.68	0.17	3.97	7.05e-05	0.052927668
IVNS1ABP	6,280.01	0.66	0.17	3.89	0.000101191	0.059782042
MRPL1	1,199.18	0.65	0.18	3.71	0.000210514	0.086554107
ZNF706	1,254.96	0.60	0.16	3.86	0.000112723	0.063199994
WASHC3	619.85	0.60	0.14	4.26	2.04e-05	0.034228732
ELFN2	52.39	−1.33	0.32	−4.12	3.74e-05	0.044827627
VAV3	94.27	−1.33	0.36	−3.66	0.000252573	0.091665894
SLC25A37	181.83	−1.38	0.38	−3.62	0.000296018	0.094923511
IRF6	107.43	−1.41	0.30	−4.71	2.43e-06	0.011632848
NAPB	23.44	−1.43	0.38	−3.75	0.000177233	0.079979834
PNOC	51.18	−1.43	0.31	−4.62	3.77e-06	0.011632848
RFX8	55.92	−1.48	0.41	−3.61	0.000307396	0.094923511
AMH	79.91	−1.51	0.33	−4.63	3.63e-06	0.011632848
LOC106739971	149.82	−1.55	0.42	−3.66	0.000251318	0.091665894
ABCB11	31.36	−1.72	0.47	−3.64	0.000268478	0.091665894
EFHD2	29.20	−1.73	0.44	−3.88	0.000103396	0.059782042
LOC109285322	15.26	−1.73	0.46	−3.74	0.00018725	0.082488257
LOC106738221	35,338.28	−1.85	0.49	−3.80	0.000147205	0.071673525
CHRNA6	11.02	−1.98	0.50	−3.99	6.62e-05	0.052927668
LOC102573842	26.51	−2.02	0.49	−4.14	3.41e-05	0.044827627
GPR4	8.96	−2.74	0.65	−4.24	2.23e-05	0.03443642
LOC102559155	910.99	−3.23	0.64	−5.08	3.83e-07	0.005763737
LOC102562759	6.98	−4.28	1.18	−3.64	0.000272491	0.091665894
LOC109282550	6.48	−4.88	1.34	−3.65	0.000261642	0.091665894
ALB	137.27	−10.39	2.79	−3.72	0.000198597	0.085452271

See Supplemental Table S3 for gene IDs and products of LOC-coded genes. lfcSE, log2FC standard error.

Enrichment analyses revealed that genes affected by hypoxia were functionally distinct from genes that displayed ontogenetic changes. Genes influenced by hypoxia generally play a role in cardiovascular physiology (cardiac muscle contraction, protein catabolism, oxygen transport, pyruvate metabolism, and adrenergic signaling), whereas ontogenetic changes in gene expression were primarily related to tissue growth and structure (cell proliferation, centromere, microtubules, and the extracellular matrix). Network analyses painted a similar picture for hypoxia-regulated genes, with interconnected gene clusters enriched for functions in the proteasome, heart contraction, and pyruvate metabolism. Network analyses of developmentally regulated genes revealed large gene clusters involved in cell division, DNA replication, and the extracellular matrix, which was consistent with enrichment analyses.

Hypoxia Stunts Embryo Growth and Causes Cardiac Hypertrophy

Incubation in hypoxic conditions restricted the overall growth of alligator embryos and decreased the absolute mass of all organs. Yet, hypoxia had differential effects on organ mass relative to body mass (i.e., hypoxia caused allometric growth of some organs). Kidney and liver mass decreased proportionally with body size (isometric growth), but heart and brain were both enlarged relative to body size (positive allometric growth). Lungs were smaller relative to body size at 70% of development (negative allometric growth) but recovered by 90% of incubation. Preferential shunting of blood and resources to certain organs during oxygen deprivation has been observed in other species (e.g., "brain sparing") (53, 55), which may be the basis for these embryonic differences.

A key finding from this study is enlargement of the heart relative to body size in hypoxic embryos. This result mirrors findings that hypoxic incubation of alligator embryos leads to increased heart mass and thickening of the right and left ventricular free walls and that hypertrophy persists into juvenile stages (36), suggesting that hypoxia induces permanent changes in the cardiovascular system. This plasticity may be adaptive, as it improves the capacity to function under hypoxic stress, as shown by enhanced cardiac power output and increased blood flow in hypoxia-exposed juveniles (36). Our study extends these findings by showing that cardiac hypertrophy in embryos is associated with specific changes in gene expression, particularly in genes related to

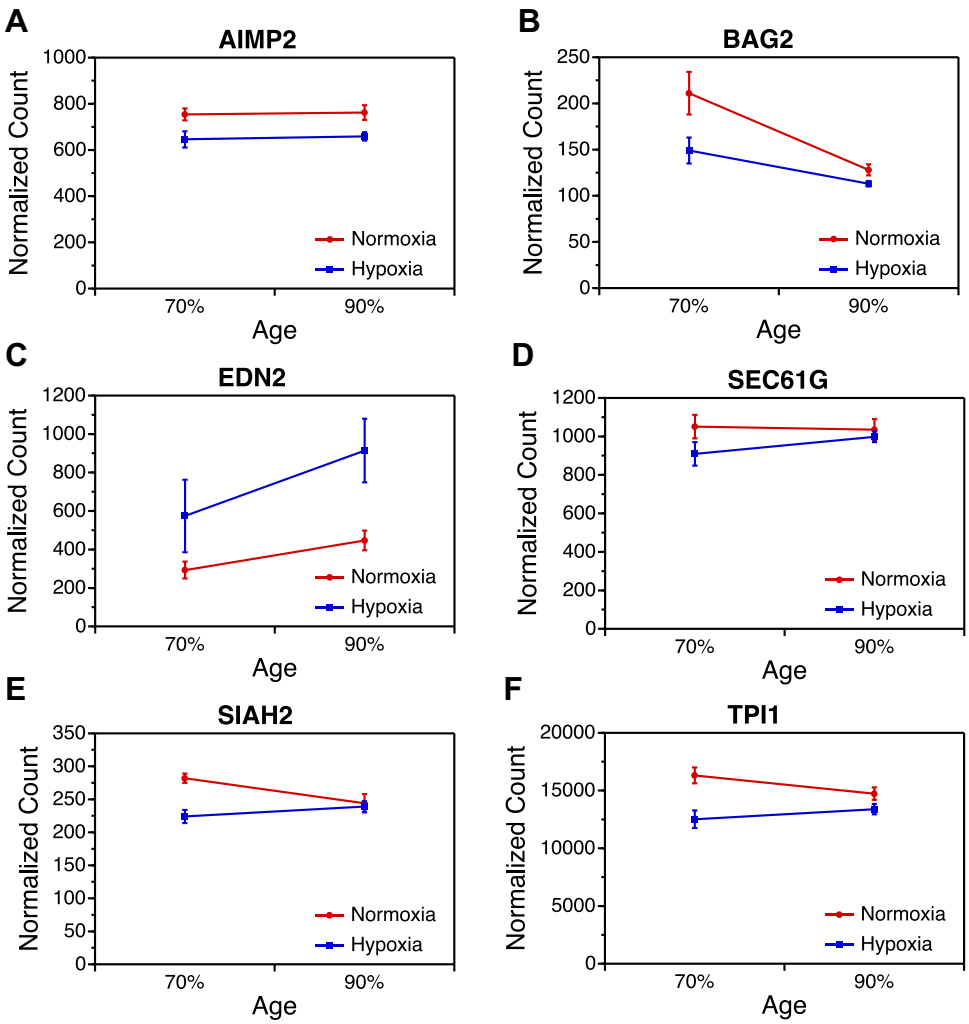

Figure 4. Gene expression patterns in the hearts of snapping turtle embryos incubated in normoxic or hypoxic conditions. Expression values are normalized counts from DESeq2 for Aminoacyl TRNA synthetase complex interacting multifunctional protein 2 (*A*), BAG cochaperone 2 (*B*), endothelin 2 (*C*), SEC61 translocon subunit gamma (*D*), Siah E3 ubiquitin protein ligase 2 (*E*), and triosephosphate isomerase 1 (TPI1) (*F*). Expression values are means (±1 SE) for each oxygen treatment group at 70% or 90% of embryogenesis. Samples sizes for 70% Normoxia ($n = 7$), 70% Hypoxia ($n = 7$), 90% Normoxia ($n = 7$), 90% Hypoxia ($n = 7$).

muscle structure and contraction, the proteasome, oxygen transport, pyruvate metabolism, and adrenergic signaling.

Although cardiac hypertrophy is often pathological in mammals, where it is associated with cardiovascular dysfunction and increased risk of ischemia-reperfusion injury (30, 31), the hypertrophic response in alligators appears to be beneficial. Hypoxic incubation shifts the cardiovascular response to acute hypoxia, enabling alligators to better tolerate low oxygen levels (38). The cardiac hypertrophy observed in our study likely contributes to enhanced hypoxia tolerance by increasing stroke volume and cardiac output, as reported in snapping turtles (34). Thus, the enlargement of the heart in response to developmental hypoxia may represent a preadaptive mechanism that primes alligators for better physiological performance in hypoxic environments encountered later in life.

Hypoxia Alters Gene Expression Patterns in Developing Hearts

Hypoxia induced significant changes in gene expression patterns in the hearts of alligator embryos, with 182 upregulated and 222 downregulated genes. Another 65 genes displayed an interaction between hypoxia and embryo age. Enrichment analyses showed that many of these genes have roles in muscle fiber structure/contraction, the proteasome, oxygen transport, pyruvate metabolism, and synaptic transmission/adrenergic signaling—functions critical for maintaining cardiac performance under hypoxic conditions. These findings align with previous research showing that developmental hypoxia significantly alters cardiovascular physiology in alligators (35–38, 54).

Comparison of hypoxia-regulated genes among alligators, humans, and mice revealed five "positive control" genes influenced by hypoxia in all three species: *AIMP2*, *BAG2*, *SEC61G*, *SIAH2*, and *TPI1*. The role of *AIMP2* and *SEC61G* in heart development has not been studied and it is not clear whether they are targets of hypoxia-inducible factors. In contrast, *SIAH2* is an E3 ubiquitin ligase that plays a pivotal role in the hypoxic response by targeting prolyl hydroxylases for degradation, leading to the stabilization and activation of hypoxia-inducible factor alpha (HIF-1α) (56). *SIAH2* also plays a role in proteasome-mediated degradation of *DCC*, a receptor critical for netrin-1-dependent cardioprotection during ischemia/reperfusion (57). Hypoxia downregulates *BAG2* mRNA and protein in ovine carotid arteries (58). Interestingly, *BAG2* plays a protective role in the heart where it compensates for *BAG3* knockout in zebrafish (59). Hypoxia also regulates expression of *TPI1* (60), a glycolytic enzyme responsible for conversion of dihydroxyacetone phosphate into glyceraldehyde-3-phosphate. Many other "positive

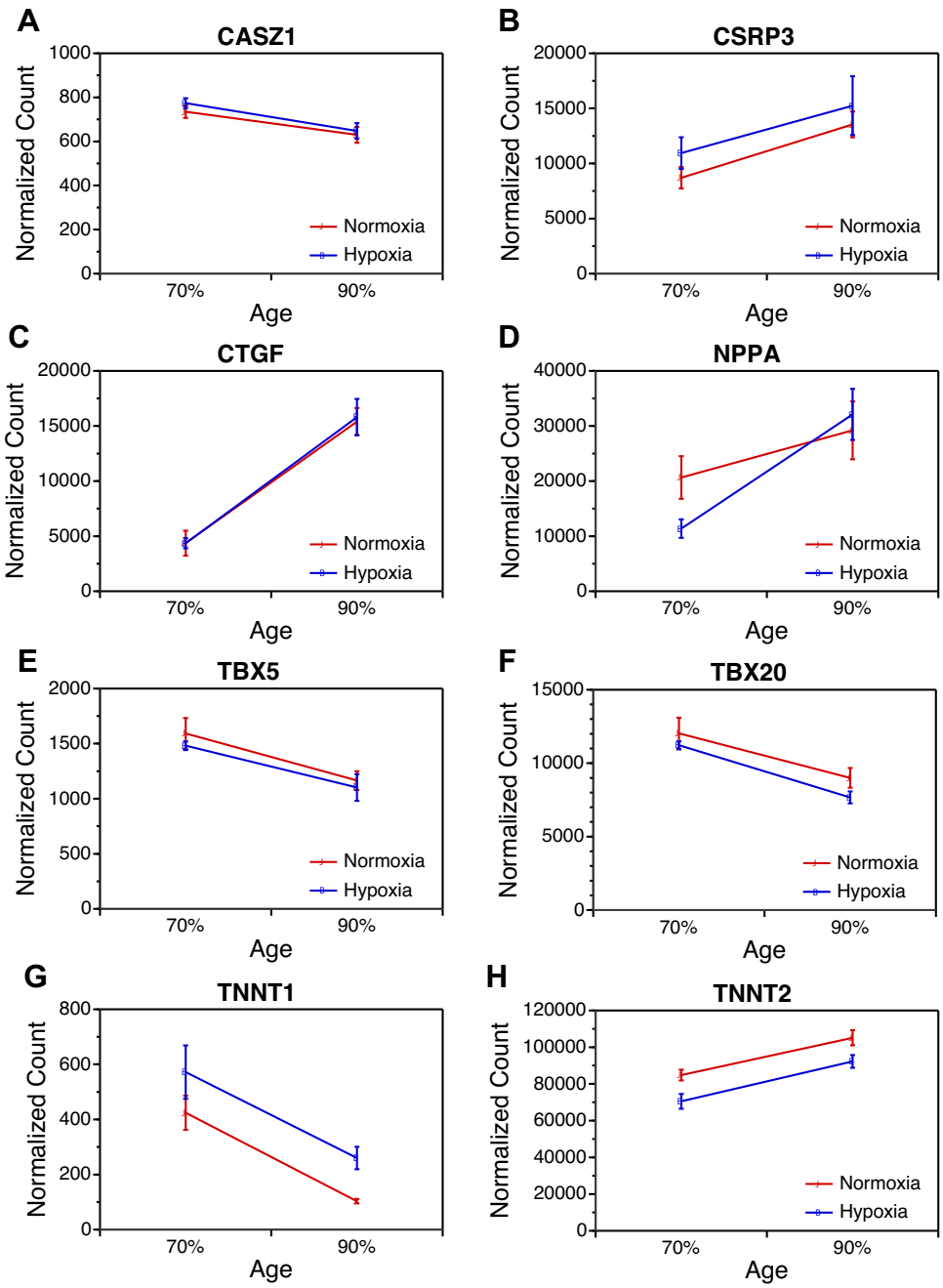

Figure 5. Gene expression patterns in the hearts of snapping turtle embryos at 70% and 90% of embryogenesis. Expression values are normalized counts from DESeq2 for castor zinc finger 1 (*A*), cysteine- and glycine-rich protein 3 (*B*), connective tissue growth factor (*C*), LOC102572997 (NPPA) (*D*), T-box transcription factor 5 (*E*), T-box transcription factor 20 (*F*), troponin T1, slow skeletal type (*G*), and troponin T2, cardiac type (*H*). Expression values are means (±1 SE) for each oxygen treatment group at 70% or 90% of embryogenesis. Samples sizes for 70% Normoxia ($n = 7$), 70% Hypoxia ($n = 7$), 90% Normoxia ($n = 7$), 90% Hypoxia ($n = 7$).

control" genes were regulated by hypoxia in alligators and one of the two mammalian species. For instance, *EDN2* is hypoxia-regulated in alligators and humans and appears to play an important role in the heart alongside its paralog *EDN1* (61). One of the most surprising findings from our comparative analysis was the limited overlap of hypoxia-regulated genes among alligators, humans, and mice (ranging from 6.3% to 16.5% of genes in pairwise comparisons). We suspect that unaccounted variation in cell type, tissue, or organ could be a major reason for the low correspondence between species. Future studies should compare hypoxia-regulated genes in the same cell type, tissue, or organ.

The Markov cluster algorithm in the STRING database revealed subnetworks of genes that were enriched for protein-protein interactions and biological/molecular functions similar to those listed earlier. Genes in several subnetworks also displayed coordinated expression patterns. For example, most genes in the largest subnetwork were downregulated in hypoxic conditions, including all 11 genes involved in proteolysis (*AKIRIN2*, *CUL2*, *HECTD3*, *SRF*, *UCHL1*, *UFD1L* and proteasome subunits *PSMA1*, *PSMA7*, *PSMB1*, *PSMD14*, *PSMD4*). Decreased proteasomal function and ubiquitination would likely alter protein turnover, leading to the accumulation of misfolded or damaged proteins. Proteomic analyses of embryonic alligator hearts also found enrichment of proteasomal proteins among differentially expressed proteins in hypoxic hearts (62). Studies in mammals suggest that impaired ubiquitin-proteosome system function contributes

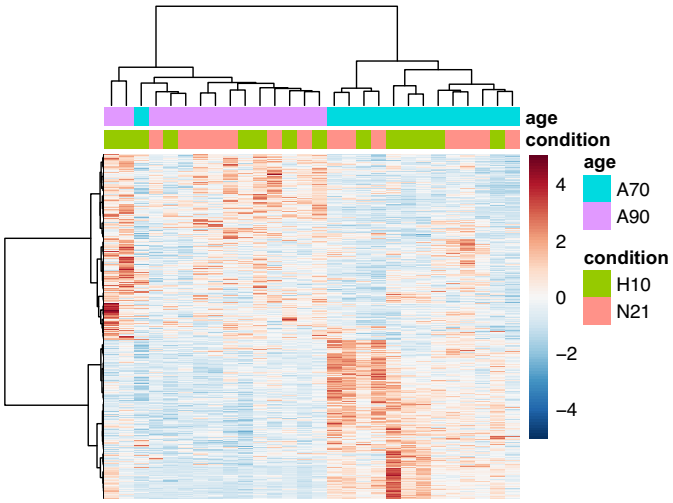

Figure 6. Heatmap of differentially expressed genes in the hearts of alligator embryos. Heatmap showing RNA sequencing (RNA-Seq) expression values for genes that were significantly affected by oxygen treatment (listed in Supplemental Table S1), embryonic age (listed in Supplemental Table S2), or the oxygen treatment by age interaction (listed in Supplemental Table S3). Expression values for genes are shown in rows, whereas individual samples are shown in columns within the heatmap. The key next to the plot shows the age and oxygen treatment for each sample.

to cardiomyopathy (63), although there is evidence that proteasome inhibition may be cardioprotective in some circumstances (64). Experimental studies using proteasome activators and inhibitors will be required to determine the specific role the proteosome plays in developing alligator hearts. In contrast, there was no consistent pattern of upregulation or downregulation of gene expression in the second largest subnetwork. This cluster of genes was not functionally enriched for any biological process but was weakly enriched for proteins with a tetratricopeptide domain. This gene cluster has no clear relationship to phenotype.

Most genes in the third largest subnetwork were downregulated by hypoxia, including eight genes involved in heart contraction, the myosin II complex, and the troponin complex. Most of these genes (*ACTC1*, *MYL2*, *MYL3*, *MYL4*, *MYL7*, *MYH7B*, and *TNNC1*) are critical components of the sarcomere, the fundamental unit of muscle contraction in the heart. Decreasing their expression would likely alter the formation and function of the sarcomeres, leading to changes in cardiomyocyte contractility (65, 66). Reduced *CKMT2* would limit the heart's energy reserves (67), further compounding the problem by making it harder for the developing heart to sustain activity, especially during periods of high demand. Decreased expression of *MYL9* could impair the development of blood vessels and smooth muscle cells that support the heart (68), potentially affecting blood flow to the heart, which could lead to cardiovascular phenotypes in later stages of development.

Most genes in the fourth subnetwork, which contained genes involved in pyruvate metabolism, were downregulated by hypoxia. Decreased expression of glycolytic and glycosylation-related genes (*GFPT2*, *MPI*, *LDHB*, and *TPI1*) could impair energy production, protein glycosylation, and metabolic flexibility. However, vertebrate hearts transition from predominately anaerobic glycolytic metabolism to oxidative phosphorylation during development (69). Thus, the decrease in expression of glycolytic genes may represent an early transition to dependence on oxidative phosphorylation in embryonic alligator hearts. In cardiac development, metabolic pathways and enzyme activities are tightly regulated to ensure proper energy production, structure formation, and function of the heart (70, 71). On the other hand, increased expression of *PDHB* may provide more energy via oxidative phosphorylation, which would be beneficial for the developing heart (72). This combination could result in metabolic and structural changes during cardiac development, leading to changes in cardiac function in later life. Indeed, juvenile alligators incubated in hypoxic conditions had reduced LEAK respiration and higher respiratory control ratios, suggesting early exposure to hypoxia-enhanced mitochondrial efficiency later in life (73). Cardiac development relies on both glycolysis and oxidative phosphorylation, and disrupting glycolysis while upregulating oxidative metabolism may be sufficient to meet the energetic and structural needs of the developing heart.

The last subnetwork of five genes was enriched for genes with translation initiation factor activity. Four of these genes were upregulated by hypoxia, whereas one gene was downregulated, but this apparent bias was not statistically significant due to the small number of genes in the cluster. Increased expression of *EIF3B*, *EIF2S3*, *EIF4A2*, and *DDX3X* would likely enhance protein synthesis, supporting cardiomyocyte proliferation, differentiation, and stress resilience during development. Proteomic analysis of embryonic alligator hearts also found enrichment of proteins involved in translation among differentially expressed proteins in hypoxic hearts (62). Taken together, coordinated changes in these subnetworks (i.e., proteasome, sarcomere, pyruvate metabolism, and translation initiation) likely contribute to cardiac hypertrophy and enhanced cardiovascular function in alligator embryos and may be a factor in the long-lasting effects of embryonic hypoxia on juvenile alligators (35–38, 54).

Ontogenetic changes in cardiac gene expression were much more extensive, with 1,960 genes upregulated and 1,584 genes downregulated as embryos developed. Several "positive control" genes that play a critical role in cardiac development during late embryogenesis in other species were developmentally regulated in the alligator. For instance, *CASZ1* encodes a transcription factor essential for cardiomyocyte proliferation, heart morphogenesis, and maturation of the cardiac conduction system (74). The *CSRP3* gene is involved in sarcomere assembly and mechanotransduction, thus ensuring cardiac contractility (75). The product of the *CTGF* gene regulates the extracellular matrix, heart valve development, and myocardial growth and can cause fibrosis when overexpressed (76, 77). *LOC102572997* (*NPPA*) encodes a key hormone in cardiac development, influencing heart size and chamber specification (78). *TBX5* and *TBX20* encode transcription factors that regulate chamber formation, septation, and conduction system development (79). *TNNT1* (the slow skeletal type of troponin) is transiently expressed in cardiac muscle but declines later in embryogenesis in mice (80), just as it does in alligator. In contrast, expression of *TNNT2* (the cardiac type of troponin) increased in alligator, consistent with its function

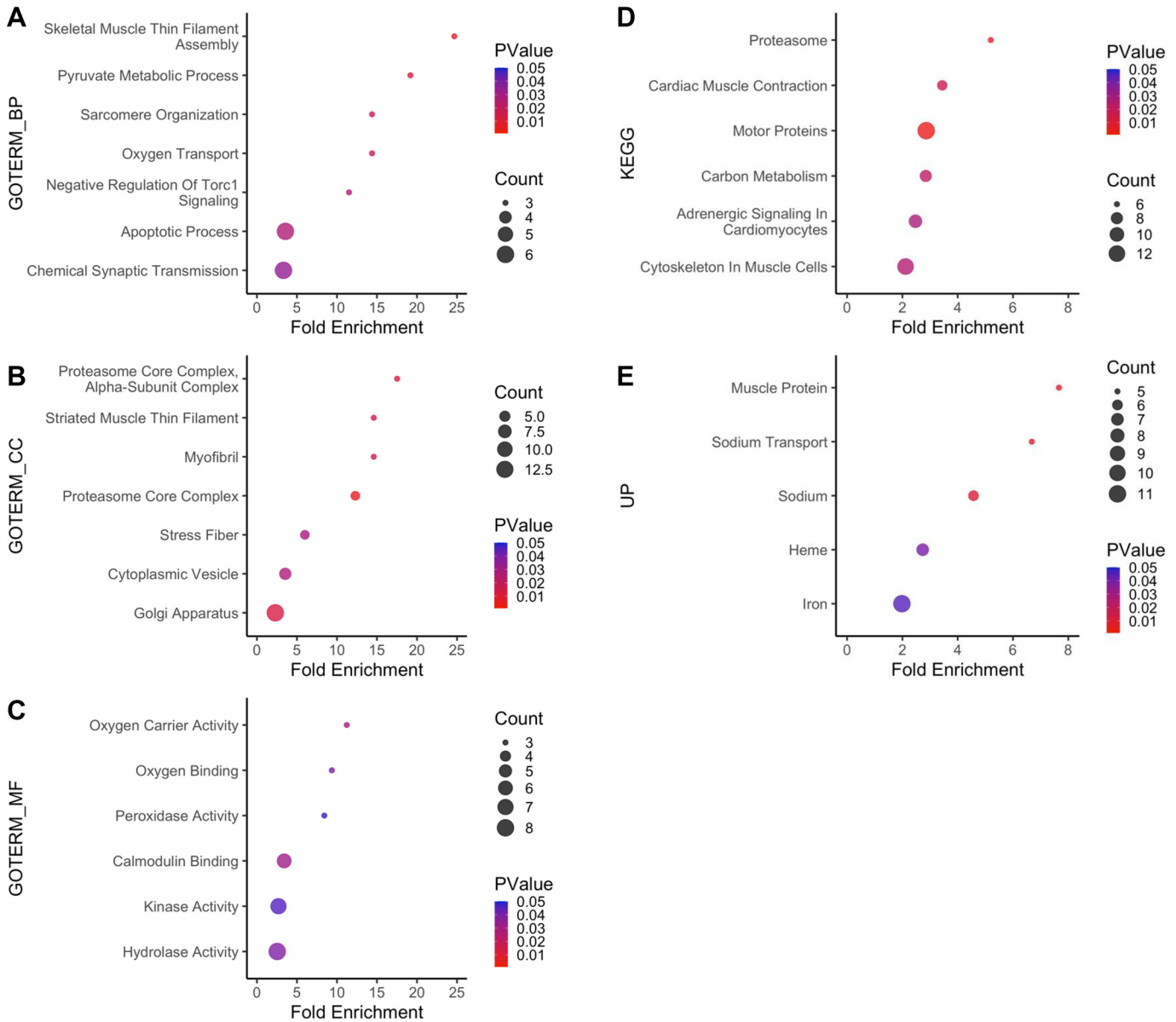

Figure 7. Enrichment analyses of hypoxia-regulated genes in the hearts of alligator embryos. Dot plots showing categories of hypoxia-regulated genes with significant functional enrichment. Genes affected by the oxygen treatment or the oxygen treatment by age interaction were compared with all alligator genes in the DAVID database. Comparisons were made using Gene Ontology (GO) terms for biological process (*A*), cellular component (*B*), and molecular function (*C*). Comparisons were also made using terms from the Kyoto Encyclopedia of Genes and Genomes (KEGG) (*D*) and the Uniprot Knowledgebase (UP) (*E*). The color of each dot represents the *P* value for each term, whereas the size of each dot represents the number of genes for each term.

in regulating calcium-dependent cardiac muscle contraction during development and throughout life (81).

Enrichment analyses showed that genes differentially expressed between 70% and 90% of embryogenesis were involved in cell division, microtubule-based movement, the extracellular matrix, and protein phosphorylation. Network analyses produced similar results, with large subnetworks of genes involved in cell division and DNA replication. Interestingly, most genes in both these subnetworks were downregulated at 90% of embryogenesis. These findings strongly suggest that cell proliferation in the heart slows as alligator embryos near the end of incubation.

Another large subnetwork of developmentally regulated genes was involved in the RHOA GTPase cycle, which influences cytoskeletal remodeling and cell contractility. Most of these genes (76%) were upregulated, suggesting that RhoA signaling increases in the heart as alligator embryos approach hatching. This finding is consistent with studies in chicken, showing RhoA is strongly upregulated in the heart (82). More broadly, RhoA has been shown to be involved in cardiomyocyte contraction, cardiac remodeling, and hypertrophy (83, 84).

The final developmentally regulated subnetwork in alligator hearts was enriched for genes involved in "regulation of blood vessel endothelial cell migration." These genes are likely involved in coronary vessel development in the alligator as they play a crucial role in angiogenesis, vascular remodeling, and cellular differentiation in mammals

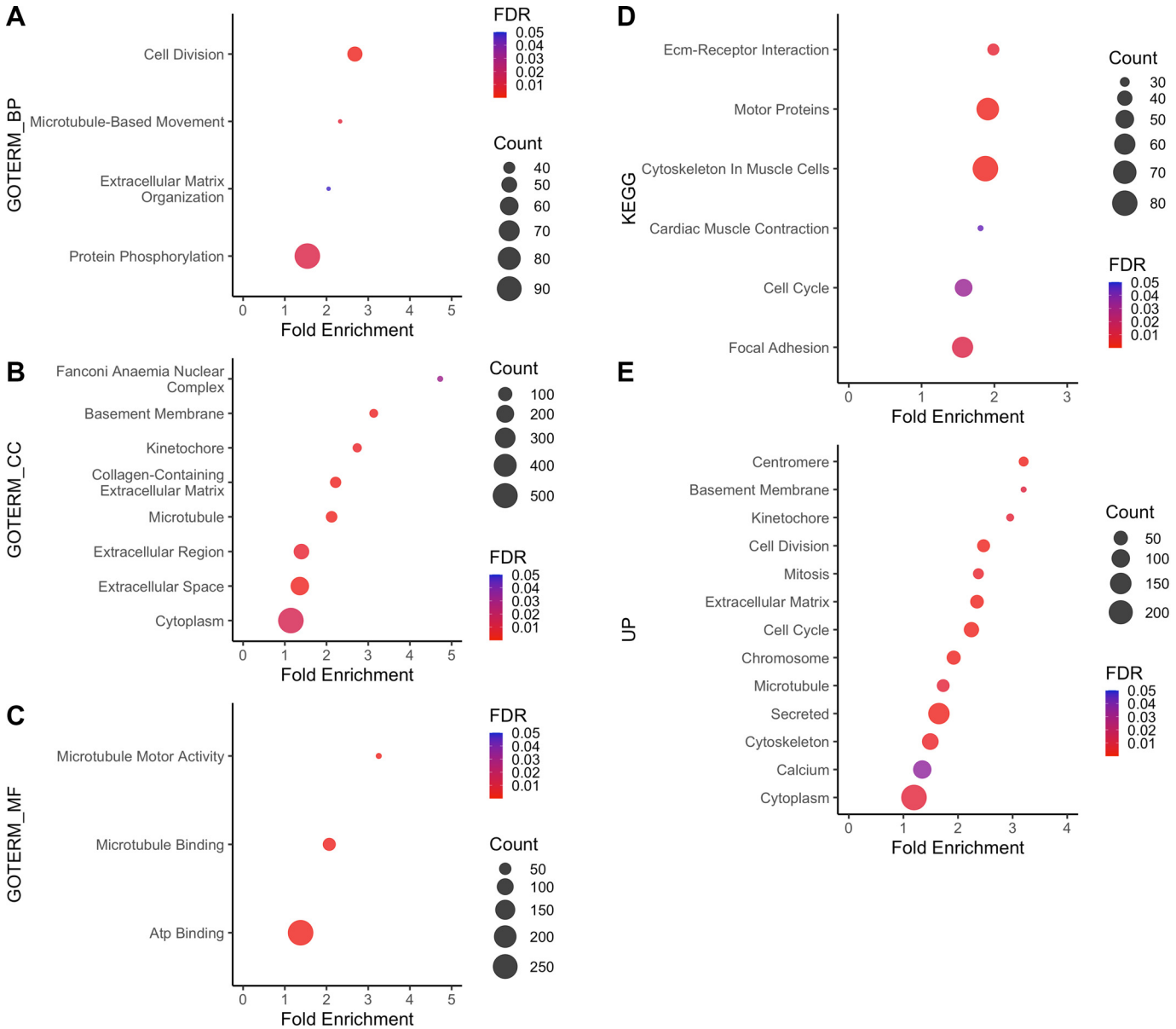

Figure 8. Enrichment analyses of genes that show developmental changes in the hearts of alligator embryos. Dot plots showing categories of developmentally regulated genes with significant functional enrichment. Genes affected by embryonic age were compared with all alligator genes in the DAVID database. Comparisons were made using Gene Ontology (GO) terms for biological process (*A*), cellular component (*B*), and molecular function (*C*). Comparisons were also made using terms from the Kyoto Encyclopedia of Genes and Genomes (KEGG) (*D*) and the Uniprot Knowledgebase (UP) (*E*). The color of each dot represents the *P* value for each term, whereas the size of each dot represents the number of genes for each term.

(85, 86). For instance, the balance of angiopoietin signaling via Tie2 receptors regulates angiogenesis, vessel maturation, and vessel stabilization (87, 88). In alligator hearts, upregulation of *ANGPT4* expression late in development would promote angiogenesis and vessel maturation, whereas *ANGPT2* upregulation and *ANGPT1* downregulation would inhibit vessel stabilization and aid sprouting.

Significance of Developmental Plasticity in Alligators

The present study highlights plasticity in cardiovascular development of alligator embryos, as demonstrated by differential gene expression and organ growth between hypoxic and normoxic conditions. Plasticity allows alligators to modify their phenotype in response to fluctuating oxygen levels in their nests, where gas composition varies due to diffusion limits, precipitation, and/or embryonic metabolism (89). Climate change and warming nest temperatures may impact oxygen availability by directly increasing metabolic rates of developing embryos, leading to higher oxygen demand (53). Temperature could also indirectly affect phenotype through its effect on sex determination (90). Warmer temperatures would also enhance microbial decomposition of organic nest materials, which could further reduce oxygen availability.

Crossley et al. (36) proposed that developmental plasticity in alligators represents a key evolutionary adaptation that

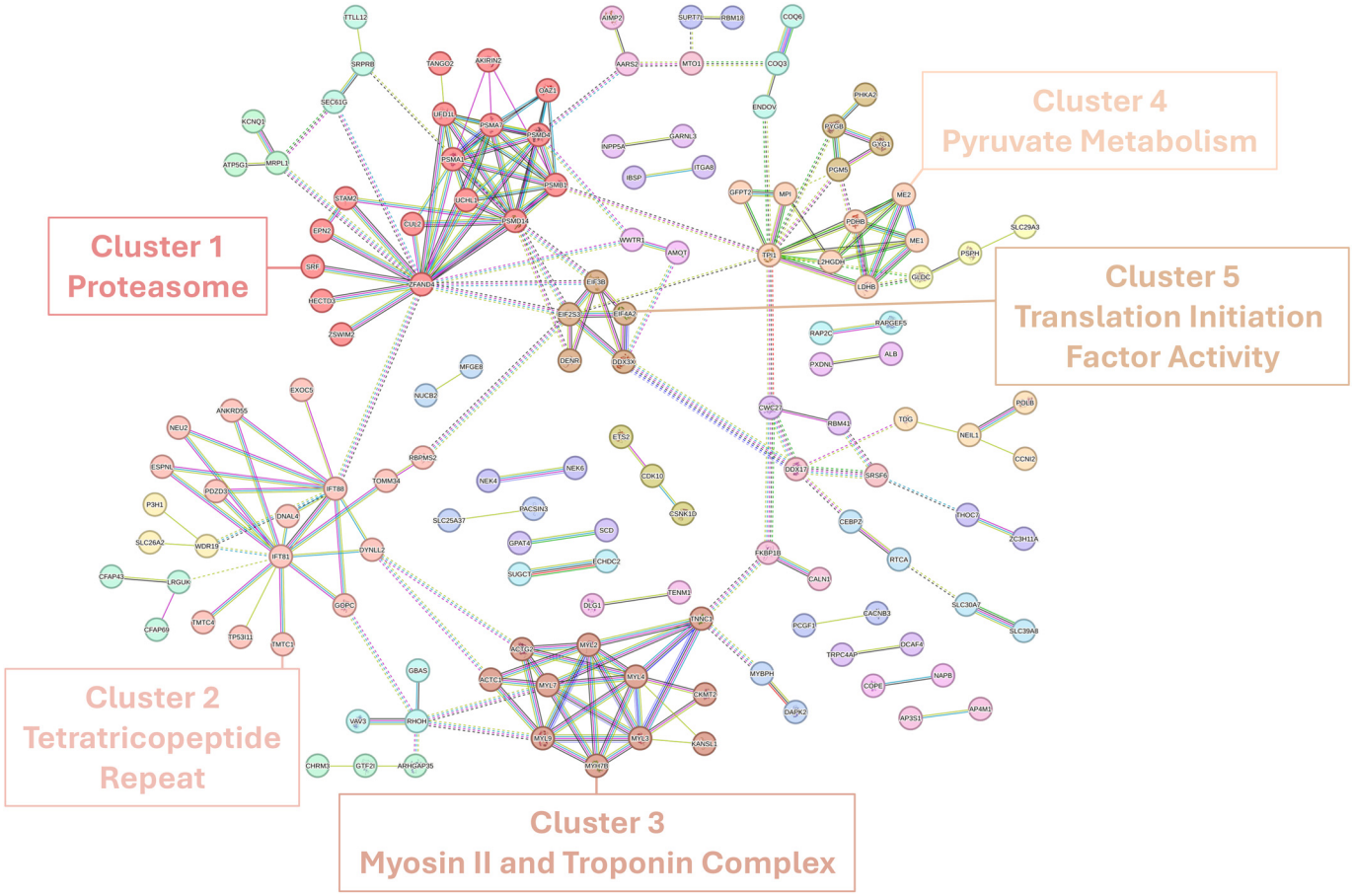

Figure 9. Network analyses of hypoxia-regulated genes in the hearts of alligator embryos. String network showing genes affected by the oxygen treatment or the oxygen treatment by age interaction. Subnetworks (i.e., clusters) of genes identified using the Markov clustering algorithm are connected by solid lines, whereas edges between subnetworks are shown by dotted lines. These subnetworks were significantly enriched for protein-protein interactions and for the terms adjacent to subnetworks.

enables better cardiovascular performance in hypoxic environments. The ability to maintain higher cardiac output and higher physiological performance under hypoxic stress suggests that developmental hypoxia serves as a preadaptive cue, programming the cardiovascular system for enhanced function later in life.

Developmental plasticity in cardiovascular phenotype in alligators is consistent with broader research on vertebrate cardiovascular development. For example, developmental hypoxia in mammals is associated with an increased risk of cardiovascular disease and hypertension in adulthood (23). However, in reptiles, hypoxia appears to have the opposite effect, promoting adaptive cardiovascular changes that enhance hypoxia tolerance (25, 34). Our findings suggest that reptiles such as alligators are capable of long-term acclimatization to hypoxia through molecular and structural modifications to their cardiovascular system.

Integration of Findings with Prior Work on Hypoxia and Cardiovascular Adaptation

Our findings align with prior research on cardiovascular effects of hypoxia in alligators. Crossley et al. (36) demonstrated that hypoxia during embryonic development causes permanent changes to the cardiovascular system, including increased heart mass and altered autonomic regulation. These changes likely improve the ability to cope with future hypoxic events. Gene expression changes observed in the current study shed light on the molecular basis for phenotypic adaptations. Specifically, coordinated changes in the expression of genes involved in muscle contraction, the proteasome, and pyruvate metabolism suggest that hypoxia induces both structural and functional modifications to the heart that may persist into later life stages.

Crossley et al. (38) showed that hypoxic incubation alters the cardiovascular response to acute hypoxia in juvenile alligators, with hypoxia-exposed individuals exhibiting enhanced stroke volume and cardiac output. These physiological changes align with the hypertrophic response observed here, suggesting that the enlarged heart size in hypoxic embryos improves cardiovascular performance. Enrichment of genes related to adrenergic signaling further suggests that hypoxia may affect autonomic regulation of the cardiovascular system, a finding supported by reports of increased sympathetic tone in hypoxia-exposed alligators (91, 92).

In conclusion, this study provides compelling evidence that developmental hypoxia alters gene expression patterns and promotes cardiac hypertrophy in American alligator embryos, likely as an adaptive mechanism to enhance

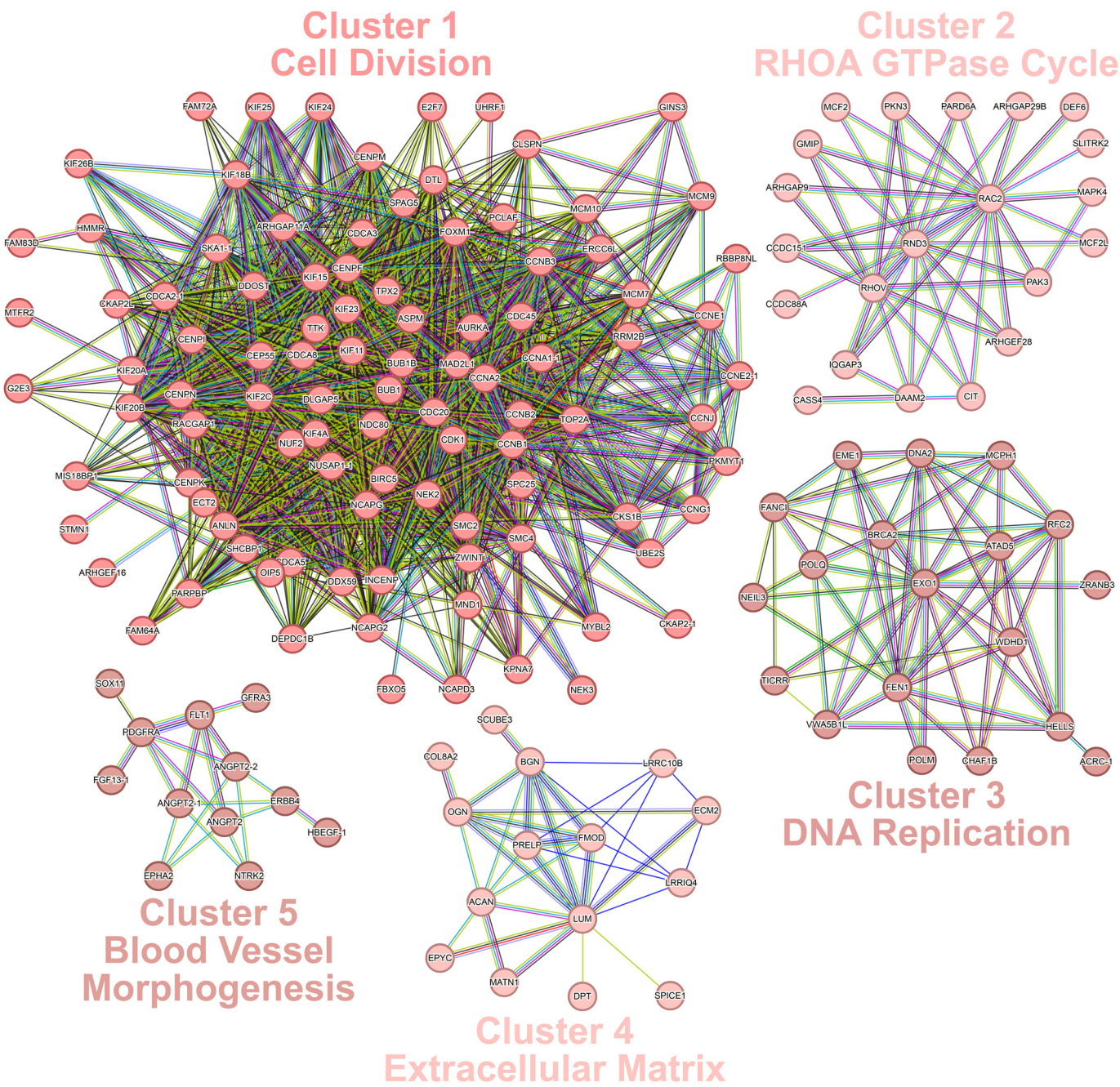

Figure 10. Network analyses of developmentally regulated genes in the hearts of alligator embryos. String network showing genes that are differentially expressed between hearts at 70% and 90% of embryogenesis at a false discovery rate (FDR) < 0.05 and > 1.5-fold change. Subnetworks (i.e., clusters) of genes identified using the Markov clustering algorithm are connected by solid lines. Only the 5 largest subnetworks are shown for clarity. Likewise, edges between subnetworks are hidden. These subnetworks were significantly enriched for protein-protein interactions and for the terms adjacent to subnetworks.

performance in low-oxygen environments. Future research should explore the functional consequences of the identified gene subnetworks and their role in shaping long-term hypoxia tolerance in alligators and other reptiles.

DATA AVAILABILITY

Data generated in the current study are available from the corresponding author on request.

SUPPLEMENTAL MATERIAL

Supplemental Tables S1–S4: https://doi.org/10.6084/m9.figshare.29332769.

ACKNOWLEDGMENTS

We thank Michael Hill for providing RNA-Sequencing support and Junguk Hur and Motoki Takaku for bioinformatics support. We thank Brandt Smith and Tiffany Millar for help maintaining the

embryos. We also thank Ruth Elsey for collecting and providing access to the alligator eggs used in the study.

GRANTS

This study was funded by the National Science Foundation of the United States Grant IOS-1755187 to (D.A.C.) and IOS-1755282 (to T.R.).

DISCLOSURES

No conflicts of interest, financial or otherwise, are declared by the authors.

AUTHOR CONTRIBUTIONS

T.R. and D.A.C. conceived and designed research; T.R. performed experiments; T.R. and T.A.C. analyzed data; T.R. and T.A.C. interpreted results of experiments; T.R. prepared figures; T.R. and D.A.C. drafted manuscript; T.R., T.A.C., and D.A.C. edited and revised manuscript; T.R., T.A.C., and D.A.C. approved final version of manuscript.

REFERENCES

1. **Pfennig DW**, **Wund MA**, **Snell-Rood EC**, **Cruickshank T**, **Schlichting CD**, **Moczek AP.** Phenotypic plasticity's impacts on diversification and speciation. *Trends Ecol Evol* 25: 459–467, 2010. doi:10.1016/j.tree.2010.05.006.
2. **Sommer RJ.** Phenotypic plasticity: from theory and genetics to current and future challenges. *Genetics* 215: 1–13, 2020. doi:10.1534/genetics.120.303163.
3. **Singh SK**, **Das D**, **Rhen T.** Embryonic temperature programs phenotype in reptiles. *Front Physiol* 11: 35, 2020. doi:10.3389/fphys.2020.00035.
4. **Bradshaw AD.** Evolutionary significance of phenotypic plasticity in plants. *Adv Genet* 13: 115–155, 1965. doi:10.1016/S0065-2660(08)60048-6.
5. **Pigliucci M.** *Phenotypic Plasticity: Beyond Nature and Nurture*. Johns Hopkins University Press, 2001.
6. **Hochachka PW**, **Somero GN.** *Biochemical Adaptation: Mechanism and Process in Physiological Evolution*. Oxford University Press, 2002.
7. **West-Eberhard MJ.** *Developmental Plasticity and Evolution*. Oxford University Press, 2003.
8. **Ghalambor CK**, **McKay JK**, **Carroll SP**, **Reznick DN.** Adaptive versus nonadaptive phenotypic plasticity and the potential for contemporary adaptation in new environments. *Funct Ecol* 21: 394–407, 2007. doi:10.1111/j.1365-2435.2007.01283.x.
9. **Müller M**, **Mentel M**, **van Hellemond JJ**, **Henze K**, **Woehle C**, **Gould SB**, **Yu RY**, **van der Giezen M**, **Tielens AG**, **Martin WF.** Biochemistry and evolution of anaerobic energy metabolism in eukaryotes. *Microbiol Mol Biol Rev* 76: 444–495, 2012. doi:10.1128/MMBR.05024-11.
10. **Mentel M**, **Tielens AGM**, **Martin WF.** Animals, anoxic environments, and reasons to go deep. *BMC Biol* 14: 44, 2016. doi:10.1186/s12915-016-0266-1.
11. **Cole DB**, **Mills DB**, **Erwin DH**, **Sperling EA**, **Porter SM**, **Reinhard CT**, **Planavsky NJ.** On the coevolution of surface oxygen levels and animals. *Geobiology* 18: 260–281, 2020. doi:10.1111/gbi.12382.
12. **Cordeiro IR**, **Tanaka M.** Environmental oxygen is a key modulator of development and evolution: from molecules to ecology. *BioEssays* 42: 2000025, 2020. doi:10.1002/bies.202000025.
13. **Hammarlund EU**, **Flashman E**, **Mohlin S**, **Licausi F.** Oxygen-sensing mechanisms across eukaryotic kingdoms and their roles in complex multicellularity. *Science* 370: eaba3512, 2020. doi:10.1126/science.aba3512.
14. **Wong W**, **Bravo P**, **Yunker PJ**, **Ratcliff WC**, **Burnetti AJ.** Examining the role of oxygen-binding proteins on the early evolution of multicellularity (Preprint). *bioRxiv* 2023.12.01.569647, 2023. doi:10.1101/2023.12.01.569647.
15. **Cummins EP**, **Strowitzki MJ**, **Taylor CT.** Mechanisms and consequences of oxygen and carbon dioxide sensing in mammals. *Physiol Rev* 100: 463–488, 2020. doi:10.1152/physrev.00003.2019.
16. **Pan YK**, **Perry SF.** Neuroendocrine control of breathing in fish. *Mol Cell Endocrinol* 509: 110800, 2020. doi:10.1016/j.mce.2020.110800.
17. **Crossley DA 2nd**, **Burggren WW**, **Reiber CL**, **Altimiras J**, **Rodnick KJ.** Mass transport: circulatory system with emphasis on nonendothermic species. *Compr Physiol* 7: 17–66, 2016. doi:10.1002/cphy.c150010.
18. **Wang T**, **Joyce W**, **Hicks JW.** Similitude in the cardiorespiratory responses to exercise across vertebrates. *Curr Opin Physiol* 10: 137–145, 2019. doi:10.1016/j.cophys.2019.05.007.
19. **Storz JF**, **Bautista NM.** Altitude acclimatization, hemoglobin-oxygen affinity, and circulatory oxygen transport in hypoxia. *Mol Aspects Med* 84: 101052, 2022. doi:10.1016/j.mam.2021.101052.
20. **Mallet RT**, **Burtscher J**, **Pialoux V**, **Pasha Q**, **Ahmad Y**, **Millet GP**, **Burtscher M.** Molecular mechanisms of high-altitude acclimatization. *Int J Mol Sci* 24: 1698, 2023. doi:10.3390/ijms24021698.
21. **Storz JF**, **Cheviron ZA.** Physiological genomics of adaptation to high-altitude hypoxia. *Annu Rev Anim Biosci* 9: 149–171, 2021. doi:10.1146/annurev-animal-072820-102736.
22. **Hickey MM**, **Simon MC.** Regulation of angiogenesis by hypoxia and hypoxia-inducible factors. *Curr Top Dev Biol* 76: 217–257, 2006. doi:10.1016/S0070-2153(06)76007-0.
23. **Giussani DA**, **Davidge ST.** Developmental programming of cardiovascular disease by prenatal hypoxia. *J Dev Orig Health Dis* 4: 328–337, 2013. doi:10.1017/S204017441300010X.
24. **Ducsay CA**, **Goyal R**, **Pearce WJ**, **Wilson S**, **Hu XQ**, **Zhang L.** Gestational hypoxia and developmental plasticity. *Physiol Rev* 98: 1241–1334, 2018. doi:10.1152/physrev.00043.2017.
25. **Galli GLJ**, **Lock MC**, **Smith KLM**, **Giussani DA**, **Crossley DA 2nd.** Effects of developmental hypoxia on the vertebrate cardiovascular system. *Physiology (Bethesda)* 38: 53–62, 2023. doi:10.1152/physiol.00022.2022.
26. **Burggren WW**, **Keller BB.** *Development of Cardiovascular Systems: Molecules to Organisms*. Cambridge University Press, 1997.
27. **Zhang L.** Prenatal hypoxia and cardiac programming. *J Soc Gynecol Investig* 12: 2–13, 2005. doi:10.1016/j.jsgi.2004.09.004.
28. **Porrello ER**, **Widdop RE**, **Delbridge LMD.** Early origins of cardiac hypertrophy: does cardiomyocyte attrition programme for pathological 'catch-up' growth of the heart? *Clin Exp Pharmacol Physiol* 35: 1358–1364, 2008. doi:10.1111/j.1440-1681.2008.05036.x.
29. **Dasinger JH**, **Davis GK**, **Newsome AD**, **Alexander BT.** Developmental programming of hypertension: physiological mechanisms. *Hypertension* 68: 826–831, 2016. doi:10.1161/HYPERTENSIONAHA.116.06603.
30. **Giussani DA.** Breath of life: heart disease link to developmental hypoxia. *Circulation* 144: 1429–1443, 2021. doi:10.1161/CIRCULATIONAHA.121.054689.
31. **Xu Y**, **Williams SJ**, **O'Brien D**, **Davidge ST.** Hypoxia or nutrient restriction during pregnancy in rats leads to progressive cardiac remodeling and impairs postischemic recovery in adult male offspring. *FASEB J* 20: 1251–1253, 2006. doi:10.1096/fj.05-4917fje.
32. **Yang Q**, **Hohimer AR**, **Giraud GD**, **Van Winkle DM**, **Underwood MJ**, **He GW**, **Davis LE.** Effect of fetal anaemia on myocardial ischaemia-reperfusion injury and coronary vasoreactivity in adult sheep. *Acta Physiol (Oxf)* 194: 325–334, 2008. doi:10.1111/j.1748-1716.2008.01892.x.
33. **Rueda-Clausen CF**, **Morton JS**, **Lopaschuk GD**, **Davidge ST.** Long-term effects of intrauterine growth restriction on cardiac metabolism and susceptibility to ischaemia/reperfusion. *Cardiovasc Res* 90: 285–294, 2011. doi:10.1093/cvr/cvq363.
34. **Ruhr I**, **Bierstedt J**, **Rhen T**, **Das D**, **Singh SK**, **Miller S**, **Crossley DA**, **Galli GL.** Developmental programming of DNA methylation and gene expression patterns is associated with extreme cardiovascular tolerance to anoxia in the common snapping turtle. *Epigenetics Chromatin* 14: 42, 2021. doi:10.1186/s13072-021-00414-7.
35. **Smith B**, **Crossley JL**, **Elsey RM**, **Hicks JW**, **Crossley DA 2nd**. Embryonic developmental oxygen preconditions cardiovascular functional response to acute hypoxic exposure and maximal β-adrenergic stimulation of anesthetized juvenile American alligators (*Alligator mississippiensis*). *J Exp Biol.* 222, 2019. doi:10.1242/jeb.205419.
36. **Crossley JL**, **Lawrence T**, **Tull M**, **Elsey RM**, **Wang T**, **Crossley DA 2nd.** Developmental oxygen preadapts ventricular function of

juvenile American alligators, Alligator mississippiensis. *Am J Physiol Regul Integr Comp Physiol* 323: R739–R748, 2022. doi:10.1152/ajpregu.00059.2022.
37. **Smith B**, **Crossley JL**, **Conner J**, **Elsey RM**, **Wang T**, **Crossley DA 2nd.** Exposure to hypoxia during embryonic development affects blood flow patterns and heart rate in juvenile American alligators during digestion. *Comp Biochem Physiol A Mol Integr Physiol* 282: 111440, 2023. doi:10.1016/j.cbpa.2023.111440.
38. **Crossley JL**, **Smith B**, **Tull M**, **Elsey RM**, **Wang T**, **Crossley DA.** Hypoxic incubation at 50% of atmospheric levels shifts the cardiovascular response to acute hypoxia in American alligators, Alligator mississippiensis. *J Comp Physiol B* 193: 545–556, 2023. doi:10.1007/s00360-023-01510-8.
39. **Puente BN**, **Kimura W**, **Muralidhar SA**, **Moon J**, **Amatruda JF**, **Phelps KL**, **Grinsfelder D**, **Rothermel BA**, **Chen R**, **Garcia JA**, **Santos CX**, **Thet S**, **Mori E**, **Kinter MT**, **Rindler PM**, **Zacchigna S**, **Mukherjee S**, **Chen DJ**, **Mahmoud AI**, **Giacca M**, **Rabinovitch PS**, **Aroumougame A**, **Shah AM**, **Szweda LI**, **Sadek HA.** The oxygen-rich postnatal environment induces cardiomyocyte cell-cycle arrest through DNA damage response. *Cell* 157: 565–579, 2014 [Erratum in *Cell* 157: 1243, 2014]. doi:10.1016/j.cell.2014.03.032.
40. **Pawlak M**, **Niescierowicz K**, **Winata CL.** Decoding the heart through next generation sequencing approaches. *Genes (Basel)* 9: 289, 2018. doi:10.3390/genes9060289.
41. **Patterson AJ**, **Zhang L.** Hypoxia and fetal heart development. *Curr Mol Med* 10: 653–666, 2010. doi:10.2174/156652410792630643.
42. **Ferguson MWJ.** Reproductive biology and embryology of the crocodilians. In: *Biology of the Reptilia: Development A*, edited by Gans C, Billett F, Maderson PFA**.** Wiley-Interscience Publication, 1985, p. 329–491.
43. **Andrews S.** FastQC: A Quality Control Tool For High Throughput Sequence Data (Online). Scientific Researcher, 2010. https://www.bioinformatics.babraham.ac.uk/projects/fastqc/ [2022 Oct 11].
44. **Ewels P**, **Magnusson M**, **Lundin S**, **Käller M.** MultiQC: summarize analysis results for multiple tools and samples in a single report. *Bioinformatics* 32: 3047–3048, 2016. doi:10.1093/bioinformatics/btw354.
45. **Bolger AM**, **Lohse M**, **Usadel B.** Trimmomatic: a flexible trimmer for Illumina sequence data. *Bioinformatics* 30: 2114–2120, 2014. doi:10.1093/bioinformatics/btu170.
46. **Kim D**, **Paggi JM**, **Park C**, **Bennett C**, **Salzberg SL.** Graph-based genome alignment and genotyping with HISAT2 and HISAT-genotype. *Nat Biotechnol* 37: 907–915, 2019. doi:10.1038/s41587-019-0201-4.
47. **Liao Y**, **Smyth GK**, **Shi W.** featureCounts: an efficient general purpose program for assigning sequence reads to genomic features. *Bioinformatics* 30: 923–930, 2014. doi:10.1093/bioinformatics/btt656.
48. **Love MI**, **Huber W**, **Anders S.** Moderated estimation of fold change and dispersion for RNA-seq data with DESeq2. *Genome Biol* 15: 550, 2014. doi:10.1186/s13059-014-0550-8.
49. **Dennis G**, **Sherman BT**, **Hosack DA**, **Yang J**, **Gao W**, **Lane HC**, **Lempicki RA.** DAVID: database for annotation, visualization, and integrated discovery. *Genome Biol* 4: P3, 2003. doi:10.1186/gb-2003-4-9-r60.
50. **Szklarczyk D**, **Kirsch R**, **Koutrouli M**, **Nastou K**, **Mehryary F**, **Hachilif R**, **Gable AL**, **Fang T**, **Doncheva NT**, **Pyysalo S**, **Bork P**, **Jensen LJ**, **von Mering C.** The STRING database in 2023: protein–protein association networks and functional enrichment analyses for any sequenced genome of interest. *Nucleic Acids Res* 51: D638–D646, 2023. doi:10.1093/nar/gkac1000.
51. **Bono H**, **Hirota K.** Meta-analysis of hypoxic transcriptomes from public databases. *Biomedicines* 8: 10, 2020. doi:10.3390/biomedicines8010010.
52. **Oliveros JC.** Venny. An Interactive Tool For Comparing Lists With Venn's Diagrams (Online). Scientific Researcher, 2007–2015. https://bioinfogp.cnb.csic.es/tools/venny/index.html.
53. **Lock MC**, **Ripley DM**, **Smith KL**, **Mueller CA**, **Shiels HA**, **Crossley DA**, **Galli GL.** Developmental plasticity of the cardiovascular system in oviparous vertebrates: effects of chronic hypoxia and interactive stressors in the context of climate change. *J Exp Biol* 227: jeb245530, 2024. doi:10.1242/jeb.245530.
54. **Crossley DA 2nd**, **Altimiras J.** Cardiovascular development in embryos of the American alligator (Alligator mississippiensis): effects of chronic and acute hypoxia. *J Exp Biol* 208: 31–39, 2005. doi:10.1242/jeb.01355.
55. **Giussani DA.** The fetal brain sparing response to hypoxia: physiological mechanisms. *J Physiol* 594: 1215–1230, 2016. doi:10.1113/JP271099.
56. **Nakayama K**, **Qi J**, **Ronai ZE.** The ubiquitin ligase Siah2 and the hypoxia response. *Mol Cancer Res* 7: 443–451, 2009. doi:10.1158/1541-7786.MCR-08-0458.
57. **Li Q**, **Wang P**, **Ye K**, **Cai H.** Central role of SIAH inhibition in DCC-dependent cardioprotection provoked by netrin-1/NO. *Proc Natl Acad Sci USA* 112: 899–904, 2015. doi:10.1073/pnas.1420695112.
58. **Goyal R**, **Longo LD.** Acclimatization to long-term hypoxia: gene expression in ovine carotid arteries. *Physiol Genomics* 46: 725–734, 2014. doi:10.1152/physiolgenomics.00073.2014.
59. **Diofano F**, **Weinmann K**, **Schneider I**, **Thiessen KD**, **Rottbauer W**, **Just S.** Genetic compensation prevents myopathy and heart failure in an in vivo model of Bag3 deficiency. *PLoS Genet* 16: e1009088, 2020. doi:10.1371/journal.pgen.1009088.
60. **Gess B**, **Hofbauer KH**, **Deutzmann R**, **Kurtz A.** Hypoxia up-regulates triosephosphate isomerase expression via a HIF-dependent pathway. *Pflugers Arch* 448: 175–180, 2004. doi:10.1007/s00424-004-1241-1.
61. **Ling L**, **Maguire JJ**, **Davenport AP.** Endothelin-2, the forgotten isoform: emerging role in the cardiovascular system, ovarian development, immunology and cancer. *Br J Pharmacol* 168: 283–295, 2013. doi:10.1111/j.1476-5381.2011.01786.x.
62. **Alderman SL**, **Crossley DA**, **Elsey RM**, **Gillis TE.** Hypoxia-induced reprogramming of the cardiac phenotype in American alligators (Alligator mississippiensis) revealed by quantitative proteomics. *Sci Rep* 9: 8592, 2019. doi:10.1038/s41598-019-45023-3.
63. **Bühringer H**, **Doroudgar S**, **Wang X**, **Frey N**, **Rangrez AY.** Editorial: Proteostasis in cardiac health and disease. *Front Mol Biosci* 11: 1433721, 2024. doi:10.3389/fmolb.2024.1433721.
64. **Pagan J**, **Seto T**, **Pagano M**, **Cittadini A.** Role of the ubiquitin proteasome system in the heart. *Circ Res* 112: 1046–1058, 2013. doi:10.1161/CIRCRESAHA.112.300521.
65. **Miyamoto SD**, **Stauffer BL**, **Sucharov CC.** Molecular pathways in cardiomyopathies. In: *Cardioskeletal Myopathies in Children and Young Adults*. Elsevier, 2017, p. 39–64.
66. **Guo Y**, **Pu WT.** Cardiomyocyte maturation: new phase in development. *Circ Res* 126: 1086–1106, 2020. doi:10.1161/CIRCRESAHA.119.315862.
67. **Park N**, **Marquez J**, **Garcia MV**, **Shimizu I**, **Lee SR**, **Kim HK**, **Han J.** Phosphorylation in novel mitochondrial creatine kinase tyrosine residues render cardioprotection against hypoxia/reoxygenation injury. *J Lipid Atheroscler* 10: 223–239, 2021. doi:10.12997/jla.2021.10.2.223.
68. **Licht AH**, **Nübel T**, **Feldner A**, **Jurisch-Yaksi N**, **Marcello M**, **Demicheva E**, **Hu J-H**, **Hartenstein B**, **Augustin HG**, **Hecker M**, **Angel P**, **Korff T**, **Schorpp-Kistner M.** Junb regulates arterial contraction capacity, cellular contractility, and motility via its target Myl9 in mice. *J Clin Invest* 120: 2307–2318, 2010. doi:10.1172/JCI41749.
69. **Rickert-Sperling S**, **Kelly RG**, **Haas N** (Editors)**.** *Congenital Heart Diseases: The Broken Heart: Clinical Features, Human Genetics and Molecular Pathways*. Springer, 365–396, 2024.
70. **Ekström A**, **Sandblom E**, **Blier PU**, **Dupont Cyr BA**, **Brijs J**, **Pichaud N.** Thermal sensitivity and phenotypic plasticity of cardiac mitochondrial metabolism in European perch, Perca fluviatilis. *J Exp Biol* 220: 386–396, 2017. doi:10.1242/jeb.150698.
71. **Sakaguchi A**, **Kimura W.** Metabolic regulation of cardiac regeneration: roles of hypoxia, energy homeostasis, and mitochondrial dynamics. *Curr Opin Genet Dev* 70: 54–60, 2021. doi:10.1016/j.gde.2021.05.009.
72. **Sun W**, **Liu Q**, **Leng J**, **Zheng Y**, **Li J.** The role of pyruvate dehydrogenase complex in cardiovascular diseases. *Life Sci* 121: 97–103, 2015. doi:10.1016/j.lfs.2014.11.030.
73. **Galli GL**, **Crossley J**, **Elsey RM**, **Dzialowski EM**, **Shiels HA**, **Crossley DA.** Developmental plasticity of mitochondrial function in American alligators, Alligator mississippiensis. *Am J Physiol Regul Integr Comp Physiol* 311: R1164–R1172, 2016. doi:10.1152/ajpregu.00107.2016.
74. **Liu Z**, **Li W**, **Ma X**, **Ding N**, **Spallotta F**, **Southon E**, **Tessarollo L**, **Gaetano C**, **Mukouyama YS**, **Thiele CJ.** Essential role of the zinc finger transcription factor Casz1 for mammalian cardiac morphogenesis

and development. *J Biol Chem* 289: 29801–29816, 2014. doi:10.1074/jbc.M114.570416.

75. **Bang ML**, **Bogomolovas J**, **Chen J.** Understanding the molecular basis of cardiomyopathy. *Am J Physiol Heart Circ Physiol* 322: H181–H233, 2022. doi:10.1152/ajpheart.00562.2021.
76. **Chuva De Sousa Lopes SM**, **Feijen A**, **Korving J**, **Korchynskyi O**, **Larsson J**, **Karlsson S**, **Ten Dijke P**, **Lyons KM**, **Goldschmeding R**, **Doevendans P**, **Mummery CL.** Connective tissue growth factor expression and Smad signaling during mouse heart development and myocardial infarction. *Dev Dyn* 231: 542–550, 2004. doi:10.1002/dvdy.20162.
77. **Daniels A**, **Van Bilsen M**, **Goldschmeding R**, **Van Der Vusse GJ**, **Van Nieuwenhoven FA.** Connective tissue growth factor and cardiac fibrosis. *Acta Physiol (Oxf)* 195: 321–338, 2009. doi:10.1111/j.1748-1716.2008.01936.x.
78. **Houweling AC**, **Van Borren MM**, **Moorman AF**, **Christoffels VM.** Expression and regulation of the atrial natriuretic factor encoding gene Nppa during development and disease. *Cardiovasc Res* 67: 583–593, 2005. doi:10.1016/j.cardiores.2005.06.013.
79. **Plageman TF**, **Yutzey KE.** Differential expression and function of Tbx5 and Tbx20 in cardiac development. *J Biol Chem* 279: 19026–19034, 2004. doi:10.1074/jbc.M314041200.
80. **Manuylov NL**, **Tevosian SG.** Cardiac expression of Tnnt1 requires the GATA4-FOG2 transcription complex. *ScientificWorldJournal* 9: 575–587, 2009. doi:10.1100/tsw.2009.75.
81. **Wei B**, **Jin JP.** TNNT1, TNNT2, and TNNT3: Isoform genes, regulation, and structure–function relationships. *Gene* 582: 1–13, 2016. doi:10.1016/j.gene.2016.01.006.
82. **Kaarbø M**, **Crane DI**, **Murrell WG.** RhoA is highly upregulated in the process of early heart development of the chick and important for normal embryogenesis. *Dev Dyn* 227: 35–47, 2003. doi:10.1002/dvdy.10283.
83. **Shimokawa H**, **Sunamura S**, **Satoh K.** RhoA/Rho-kinase in the cardiovascular system. *Circ Res* 118: 352–366, 2016. doi:10.1161/CIRCRESAHA.115.306532.
84. **Kilian LS**, **Voran J**, **Frank D**, **Rangrez AY.** RhoA: a dubious molecule in cardiac pathophysiology. *J Biomed Sci* 28: 33, 2021. doi:10.1186/s12929-021-00730-w.
85. **Reese DE**, **Mikawa T**, **Bader DM.** Development of the coronary vessel system. *Circ Res* 91: 761–768, 2002. doi:10.1161/01.res.0000038961.53759.3c.
86. **Tian X**, **Zhou B.** Coronary vessel formation in development and regeneration: origins and mechanisms. *J Mol Cell Cardiol* 167: 67–82, 2022. doi:10.1016/j.yjmcc.2022.03.009.
87. **Suri C**, **Jones PF**, **Patan S**, **Bartunkova S**, **Maisonpierre PC**, **Davis S**, **Sato TN**, **Yancopoulos GD.** Requisite role of angiopoietin-1, a ligand for the TIE2 receptor, during embryonic angiogenesis. *Cell* 87: 1171–1180, 1996. doi:10.1016/s0092-8674(00)81813-9.
88. **Augustin HG**, **Koh GY**, **Thurston G**, **Alitalo K.** Control of vascular morphogenesis and homeostasis through the angiopoietin–Tie system. *Nat Rev Mol Cell Biol* 10: 165–177, 2009. doi:10.1038/nrm2639.
89. **Grigg G**, **Thompson M**, **Beard L**, **Harlow P.** Oxygen levels in mound nests of Crocodylus porosus and Alligator mississippiensis are high, and gas exchange occurs primarily by diffusion, not convection. *Australian Zoologist* 35: 235–244, 2010. 2010. doi:10.7882/AZ.2010.012.
90. **Alvine T**, **Rhen T**, **Crossley DA.** Temperature-dependent sex determination modulates cardiovascular maturation in embryonic snapping turtles Chelydra serpentina. *J Exp Biol* 216: 751–758, 2013. doi:10.1242/jeb.074609.
91. **Joyce W**, **Miller TE**, **Elsey RM**, **Wang T**, **Crossley DA.** The effects of embryonic hypoxic programming on cardiovascular function and autonomic regulation in the American alligator (Alligator mississippiensis) at rest and during swimming. *J Comp Physiol B* 188: 967–976, 2018. doi:10.1007/s00360-018-1181-2.
92. **Smith B**, **Crossley JL**, **Elsey RM**, **Hicks JW**, **Crossley DA.** Embryonic developmental oxygen preconditions cardiovascular functional response to acute hypoxic exposure and maximal β-adrenergic stimulation of anesthetized juvenile American alligators (Alligator mississippiensis). *J Exp Biol* 222: jeb205419, 2019. doi:10.1242/jeb.205419.